Thermobar: An Open-Source Python3 Tool for Thermobarometry and Hygrometry

Penny E. Wieser[‡], Maurizio Petrelli[§], Jordan Lubbers[¶], Eric Wieser[‖], Sinan Ozaydin[*], Adam Kent[†], Christy Till[‡‡]

This is a non-peer reviewed manuscript uploaded to EarthArxiv (submitted to Volcanica)

We welcome feedback of any kind – we want the paper to be as good as possible (e.g. spotting typos, or new features you want to see in Thermobar)

@Penny_wieser (Twitter)

penny_wieser@berkeley.edu

VOLCANICA

Thermobar: An Open-Source Python3 Tool for Thermobarometry and Hygrometry

Penny E. Wieser[‡], Maurizio Petrelli[§], Jordan Lubbers[¶], Eric Wieser[‖], Sinan Ozaydin[*,**], Adam Kent[†,††], Christy Till[‡‡]

Abstract

We present Thermobar, a new open-source Python3 package for calculating pressures, temperatures, and melt compositions from mineral and mineral-melt equilibrium. Thermobar allows users to perform calculations with >100 popular parametrizations involving liquid, olivine-liquid, olivine-spinel, pyroxene only, pyroxene-liquid, two pyroxene, feldspar-liquid, two feldspar, amphibole only, amphibole-liquid, and garnet equilibria. Thermobar is the first open-source tool which can match up all possible pairs of phases from a given region, and apply various equilibrium tests to identify pairs from which to calculate pressures and temperatures (e.g., pyroxene-liquid, two pyroxene, feldspar-liquid, two feldspar, amphibole-liquid). Thermobar also contains functions allowing users to propagate analytical errors using Monte-Carlo methods, convert pressures to depths using different crustal density profiles, plot mineral classification and mineral-melt equilibrium diagrams, calculate liquid viscosities, and convert between oxygen fugacity values, buffer positions and Fe speciation in a silicate melt. Thermobar can be downloaded using pip and extensive documentation is available at https://thermobar.readthedocs.io/.

1 Introduction

Determining the pressures and temperatures of formation or equilibration of igneous phases in the Earth's crust and mantle (thermobarometry), and the melt compositions from which these phases grew (hygrometry and chemometry), is critical for understanding the behavior of magmatic systems, and for placing them in their geodynamic and tectonic contexts. Estimates of temperature have been used by a wide range of petrologic studies to investigate many important questions in igneous petrology, including the long-term temperature evolution of magmas (e.g. Rout et al. [2021], Szymanowski et al. [2017], Bachmann and Dungan [2002]), distinguishing between primary and recycled magmatic crystals (Walker et al. [2013]), interpreting magma reservoir dynamics (e.g., Evans et al. [2016], Caricchi et al. [2020]), and constraining timescales of magmatic processes (e.g., Mutch et al. [2021], Cooper [2019], Shamloo and Till [2019]). Similarly, estimating the pressure of magmatic processes is also fundamental to our understanding of igneous processes. Evaluating magma storage depths in arcs plays a vital role in determining the growth, chemical, and structural evolution of the Earth's crust (e.g., Rudnick [1995], Lee and Anderson [2015], Ducea et al. [2015]). Precisely constraining magma storage depths beneath active volcanic centers helps to inform risk evaluation during periods of volcanic unrest (Andrews et al. [2019], Pritchard et al. [2019], Stock et al. [2018]). Hygrometry, which calculates the H_2O content of melts, is vital for understanding differences in eruptive behavior and the processes triggering eruptions (Stock et al. [2016], Waters and Lange [2015]), as well as to place constraints on melt properties such as viscosity and temperature. Finally, chemometry uses the composition of mineral phases to estimate melt major element contents, which can provide insights into the range of magma compositions fractionating within a given volcanic system (Zhang et al. [2017]).

Mineral and mineral-melt barometers, thermometers, hygrometers and chemometers are based on the thermodynamics of the reactions that occur in igneous systems. For example, equilibria with significant volume differences between prod-

[*]College of Earth, Ocean and Atmospheric Sciences, Oregon State University
[†]Department of Earth and Planetary Sciences, UC Berkeley
[‡]Corresponding author: penny_wieser@berkeley.edu
[§]Department of Physics and Geology, University of Perugia
[¶]College of Earth, Ocean and Atmospheric Sciences, Oregon State University
[‖]Department of Engineering, Cambridge University
[**]School of Natural Sciences, Macquarie University
[††]College of Earth, Ocean and Atmospheric Sciences, Oregon State University
[‡‡]School of Earth and Space Exploration, Arizona State University

ucts and reactants are sensitive to pressure, whereas those with entropy differences are sensitive to temperature. Specific phase equilibrium are also sensitive to melt H_2O content, so act as hygrometers (e.g., Waters and Lange [2015]), and silicate melt composition (chemometers). In reality, while thermodynamics is often used to determine which components are expected to correlate with pressure, temperature or water content, equations are normally calibrated empirically or semi-empirically.

While a number of alternative methods exist to estimate magma storage pressures (e.g., geophysical studies, melt inclusion saturation depths), mineral-only and mineral-melt barometry remains one of the most versatile. Unlike geophysical methods, mineral barometry can be applied to volcanoes with no ground based monitoring equipment, to quiescent, dormant, extinct, and heavily eroded volcanic systems, and to deposits deep in the geological record. Additionally, unlike melt inclusion studies which rely on the collection of rapidly-cooled tephra samples to minimise H_2O-loss and crystallization of the melt inclusion, mineral barometers can be applied to tephra, slowly cooled lava flows, and igneous intrusions. Similarly, although mineral-melt hygrometry provides a less direct measure of H_2O contents than measurements of melt inclusions or H^+ measurements in minerals, it is an invaluable tool in extrusive rocks which have undergone cooling which is sufficiently slow that melt inclusions and minerals have likely lost their H^+ by diffusion (Gaetani et al. [2012]). Finally, a near absence of alternative methods to determine temperatures of magmatic storage means that mineral-melt thermometry is a very widely-used technique. The wide utility of barometry, thermometery and hygrometry is reflected in the hundreds of different expressions relating the composition of igneous phases to intensive parameters such as T, P, H_2O and melt composition. There have also been a number of papers assessing their relative strengths and pitfalls, and tweaking older models when new data emerges. In particular, the review of Putirka [2008] summarized the most popular thermobarometers, and provided a number of new equations calibrated on experimental data available in LEPR (library of experimental phase relations, Hirschmann et al. [2008]). Alongside this review, K. Putirka released a series of Excel workbooks,currently available at: http://www.fresnostate.edu/csm/ees/faculty-staff/putirka.html. These spreadsheets are widely used by the community to perform thermobarometry calculations. New thermometers published since this review are available as Excel spreadsheets (e.g., Pu et al. [2017], Masotta et al. [2013]), Excel spreadsheets and Python scripts (e.g., Brugman and Till [2019]), or Excel spreadsheets and Matlab scripts (e.g., Waters and Lange [2015]). However, a number of other models have no publicly-available tool (e.g., Sugawara [2000], Mutch et al. [2016]), although spreadsheets can sometimes be obtained upon request through the authors. This myriad of different calculators, with different input and output structures, means that performing calculations on a variety of different mineral species within a given volcanic system is very time consuming, and requires users to repeatedly reformat their chemical data. The fact that results from different equations can't be easily compared within a single tool has hindered detailed comparisons between models. There is also often little independent quality control or benchmarking, so numerous supplementary spreadsheets contain errors (and there is no good version control once these errors are fixed).

Additionally, a number of methods have been developed in recent years which are very difficult to perform in a spreadsheet. For example, it is common that only a narrow range of liquid composition will be erupted in any given episode/phase of a volcanic system, while the erupted crystal cargo may be very chemically diverse, having grown from a range of melt compositions undergoing chemical differentiation at depth. Thus, it is very challenging to identify which minerals grew or equilibrated with which melts in order to perform meaningful thermobarometric calculations.

One solution to this problem was developed by Winpenny and Maclennan [2011], who considered all possible pairings of erupted Cpx compositions from a single flow (Borgarhraun, Iceland) with a compilation of 1000 whole-rock and glass analyses from other Icelandic eruptions. They only perform thermobarometry on Cpx-Liq pairs in equilibrium based on Fe-Mg and trace element partitioning laws. This method was adapted by Neave and Putirka [2017], who used filters assessing the degree of equilibrium in terms of the Enstatite-Ferrosilite (EnFs), Calcium-Tschermak (CaTs) and Diopside-Hedenbergite (DiHd) components as well as Fe-Mg equilibrium (but didn't use trace elements). These "melt matching" methods are powerful but are unsuited to spreadsheet calculations; evaluating all possible pairs for 1000 liquids and 200 Cpx would require a spreadsheet with 200,000 rows. In addition, many of these calculations are iterative, so P-T and equilibrium parameters must be cosolved. For example, assessing Fe-Mg equilibrium requires knowledge of the temperature, which in turn requires knowledge of the pressure. This makes these calcuations very computationally expensive. Although different scripting-based solutions have been developed for calculations of this type, none are publicly available at the time of writing, or particularly computationally efficient (taking tens of minutes to assess several hundred Cpx-Liq

List of Abbreviations

P	Pressure
T	Temperature
Ol	Olivine
Liq	Liquid
Cpx	Clinopyroxene
Opx	Orthopyroxene
Fspar	Feldspar
Plag	Plagioclase Feldspar
Kspar	Potassium Feldspar
Amp	Amphibole
Sp	Spinel
K_D	Distribution coefficient of Fe-Mg between Phase 1 and Phase 2
DiHd	Diopside-Hedenbergite
EnFs	Enstatite-Ferrosilite
CaTs	Ca-Tschermak's
Jd	Jadiete

List of Python Jargon

Pandas (pd.)	A python package allowing handling of spreadsheet-like data structures
NumPy (np.)	A python package that handles the underlying math of most calculations (E.g., log, exp)
Matplotlib (plt.)	A python library used for plotting
string	Pieces of text
float	A single number that is not an integer
integer	A single number that is an integer
Pandas Series	A 1D column of data.
Pandas DataFrame	A 2D data structure (labelled column headings, rows). Can visualize as a collection of pandas series (like a single sheet in an excel spreadsheet).
Dictionary	Look up tables from one value to another. In Thermobar, they are frequently used to store multiple pandas dataframes, each associated with a specific "key". These dataframes can be thought of as separate sheets in a single Excel spreadsheet (i.e. the dictionary) with the key corresponding to the sheet name.

Figure 1: List of abbreviations

pairs).

Existing tools also have no efficient way to propagate uncertainties in input parameters (e.g. using Monte Carlo methods) without having to manually duplicate thousands of rows. This has meant that there has been very limited assessment of the true errors associated with thermobarometry.

2 Thermobar: An open-source solution

To address the shortage of user-friendly tools for performing popular and advanced calculations, we present a new software tool Thermobar, written in the open-source language Python3 (which is growing in popularity within the Earth Sciences; Petrelli [2021]). Thermobar focuses on thermobarometery, hygrometry and chemometry applicable to the crystallization of igneous phases from silicate melts within the crust and upper mantle, including >100 expressions relating to equilibrium for liquid, olivine-liquid, olivine-spinel, pyroxene, pyroxene-liquid, amphibole, amphibole-liquid, garnet, feldspar and feldspar-liquid equilibrium (Fig. 2). The full list of thermometers, barometers, and hygrometers available in Thermobar, along with the relevant functions and names used to select these equations in Thermobar, are summarized in Figures 8-12 at the end of this manuscript.

We do not consider parameterizations calculating the conditions at which primitive liquids last equilibrated with their mantle sources (see Till [2017]). Based on the complexities associated with the local installation of thermodynamic software tools, we also don't provide calculation tools for geothermobarometers developed using rhyoliteMELTS as a framework (e.g., Gualda and Ghiorso [2014], Harmon et al. [2018], thermodynamic models of Fe-Ti oxides relying on ThermoEngine, (Ghiorso and Prissel [2020]), or thermobarometers used heavily within the field of metamorphic petrology, many of which rely on THERMOCALC (Powell et al. [1998]).

For maximum versatility, Thermobar allows users to easily swap between different barometry, thermometry and hygrometry equations, and to iterate towards a solution when the system is underconstrained (e.g. iterating pressure and temperature, H_2O contents and temperature). Additionally, we provide a number of functions for assessing equilibrium, mineral-liquid and mineral-mineral matching, and Monte-Carlo error propagation. Thermobar has been extensively benchmarked to demonstrate that it gives the same results as existing tools (see https://github.com/PennyWieser/Thermobar/tree/main/Benchmarking).

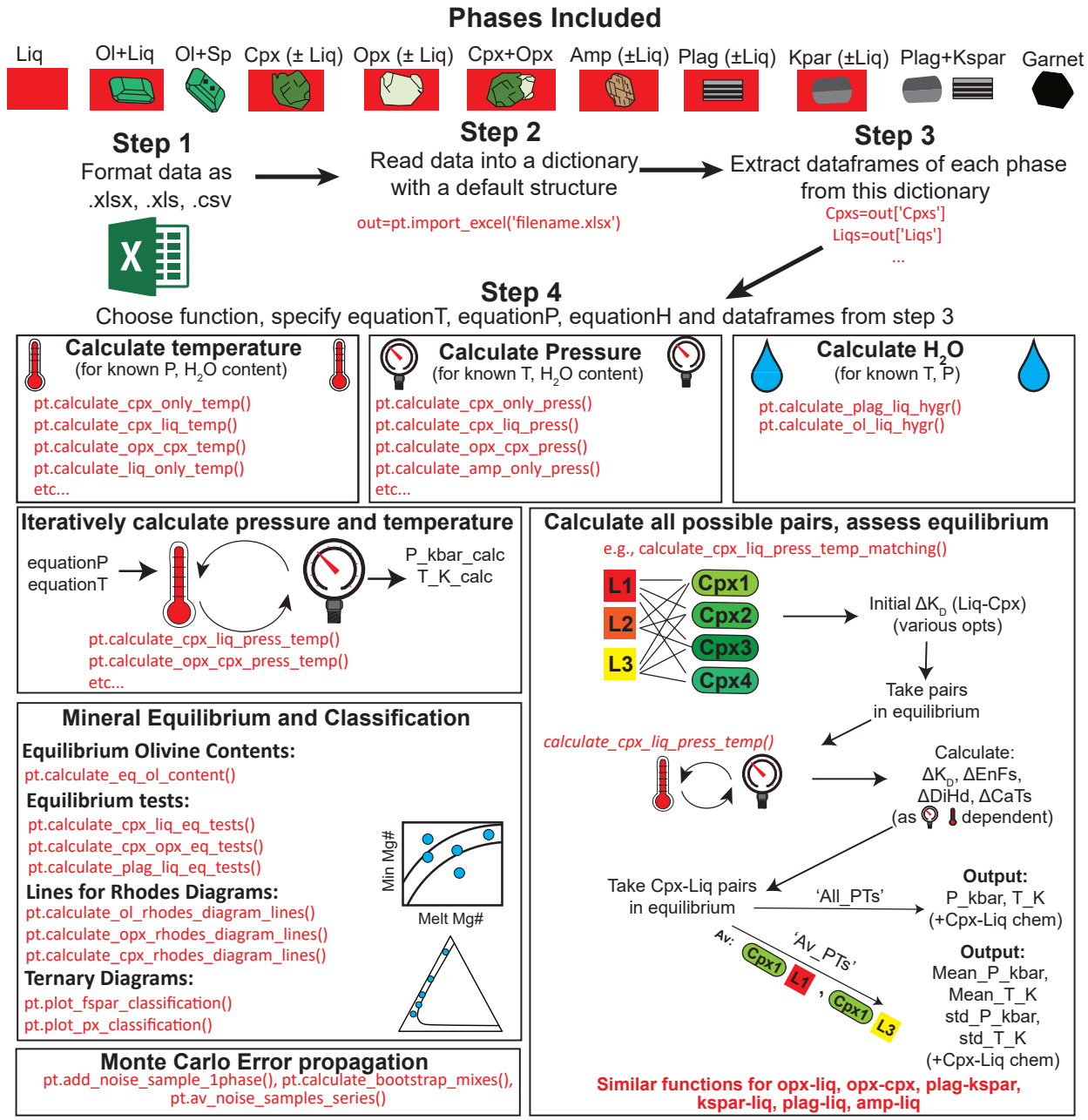

Figure 2: Schematic of some of the functions available in Thermobar. Thermobar reads in data supplied from a spreadsheet-type format. The `import_excel` function returns data as separate dataframes for each phase, combined into a single dictionary. Once extracted from this dictionary, these dataframes can be fed into a number of different functions. In addition to simple calculations of T, P and H_2O content, Thermobar allows users to iterate different equations for pressure and temperature, assess all possible matches for pairs of phases, and many other useful functions for petrologists.

3 Thermobar structure

3.1 Installation

Thermobar can be installed locally on Python versions >=3.7 using the command from either the command prompt (Windows) or the terminal (Mac):

```
pip install Thermobar
```

For python beginners, we recommend using Jupyter environments (e.g. Jupyter Lab and Jupyter Notebook), in which case, Thermobar can be installed in a similar way within a code cell (with an additional !):

```
!pip install Thermobar
```

After installation, the user must load Thermobar into their script (here we load Thermobar as pt, but users could choose any letters they wish):

```
import Thermobar as pt
```

Any function from Thermobar is then called by typing the chosen abbreviation, followed by a dot, followed by the function name:

```
pt.function_name
```

For example, to use the function to calculate liquid-only temperatures, the user would type the following:

```
pt.calculate_liq_only_temp(args)
```

With input variables (termed arguments, or args) required by the function inside the brackets.

Documentation for each function, including information on the required input variables, can be accessed using the help feature:

```
help(pt.calculate_liq_only_temp)
```

3.2 Python terminology

Thermobar makes extensive use of Numpy (Harris et al. [2020]) and Pandas (pandas development team [2020]). For the plots shown in this paper, the plotting library matplotlib is used (Hunter [2007]). We recommend importing all these packages along with Thermobar at the start of the script (see Fig. 3):

```
import numpy as np
import pandas as pd
import matplotlib.pyplot as plt
```

Five main types of data are used in Thermobar (Fig. 1):

1. "strings" are pieces of text (e.g., choosing which equation to use in a function - equationP="P_Put2008_eq30").

2. Floats and integers are numbers, such as specifying P=5 (integer) or P=5.5 (float) to perform calculations at 5 kbar and 5.5 kbar respectively.

3. pandas.Series can be thought of as a single column of data (like a single column in an Excel spreadsheet).

4. pandas.Dataframes are like a single sheet in Excel, comprising of columns with clear column headings (and are a collection of pandas.Series).

5. Dictionaries are look up tables from one value to another. In Thermobar, they are frequently used to store multiple pandas dataframes, each associated with a specific "key". These dataframes can be thought of as separate sheets in a single Excel spreadsheet (i.e. the dictionary), with the key corresponding to the sheet name.

3.3 Data Input

Users should format their compositional data as an Excel spreadsheet (.xlsx, .xls) or a comma separated values (.csv) file, with each analysis having its own row, and oxide components in wt% oxide as column headings (Fig. 3). The order of columns doesn't matter, as the python pandas package will identify the column heading regardless of its location. This spreadsheet can be imported into Thermobar using the `import_excel` function, which recognises different phases based on the presence of an underscore followed by a phase identifier in column headings. For example, the column heading SiO2_Liq tells the code that this is the column containing the SiO_2 content of the liquid/melt phase.

To have the sample ID returned along with the oxides, these names should be stored in a column with the heading "Sample_ID_Cpx", "Sample_ID_Opx" etc. The full list of phase identifiers to use in headings is given below:

- Liquid (_Liq)
- Clinopyroxene (_Cpx)
- Orthopyroxene (_Opx)
- Plagioclase (_Plag)
- Alkali feldspar (_Kspar)
- Spinel (_Sp)
- Amphibole (_Amp)
- Garnet (_Gt)

If only a single phase composition is being loaded at each time (e.g. just Liq compositions), there is no need for users to add "_Liq" to each column heading. They can simply specify this suffix in the `import_excel` function itself, which appends the suffix onto every column name:

```
pt.import_excel('FileName.xlsx',
sheet_name='Sheet1', suffix="_Liq")
```

Thermobar also has a function `import_excel_err` which recognises columns of the form SiO_2_Cpx_Err. These errors can be absolute values (in wt%) or percentage errors (users specify the error type in the function `pt.add_noise_sample_1phase`, which generates synthetic distributions of analyses).

Both import functions read from the selected Excel spreadsheet, and arrange the columns into a dataframe for each mineral phase. To address the fact that many literature datasets have text values (strings) in certain cells (e.g., bdl, n.d, NA, N/A), Thermobar automatically replaces any string in any oxide column with a zero. If a given column heading Thermobar is expecting is absent, Thermobar makes this column, then fills it with zeros. For simplicity, and to create a uniform output structure, if the input spreadsheet only contains columns with the headings "_Liq", the returned dataframes for other phases will consist entirely of zeros.

The dataframes for all recognised phases are joined into a pandas dictionary (named "out" in Fig. 3). The dataframes for each phase are accessed from this output using `dictionary_name['Phase_name']` (see Step 2, Fig. 3), where phase names are the same as the column identifiers used in the input spreadsheet, with the addition of an "s". For example, `out['Cpxs']` returns the dataframe of Cpx in Fig. 3. We recommend that these dataframes are inspected before proceeding using the .head() function, which displays the first 5 rows. Column heading for oxides that were not recognised will be filled with zeros (perhaps due to unusual characters in oxide names, decimal points other than full stops (.), or spaces before the column name in Excel. Inspecting outputs at this stage allows these issues to be identified.

In addition to "recognised" oxide column headings with specified phase identifiers, users can have any other column names they wish. For example, for thermometry calculations, users may want to use a pressure derived from other sources, or metadata like latitude, depth within a unit, etc. In Fig. 3, pressure is entered in a column labelled "P_kbar_MIs", which records the average pressure calculated from melt inclusions from the same sample. The exact name doesn't matter; a dataframe is present in the output dictionary named "my_input" which contains all columns from the original spreadsheet, and these additional column can be accessed at any time using `my_input['Column_name']`.

3.4 Units

Thermobar performs all calculations using temperature in Kelvin, pressure in kbar, and chemistry in wt% for inputs, and the same units for outputs. The only exception is that Ni in garnet is entered in ppm.

3.5 Fe redox

For liquids, Thermobar allows users to specify how they partition Fe between ferrous and ferric iron, because equilibrium tests involving the partitioning of Fe^{2+} and Mg between minerals and melt are sensitive to the proportion of Fe^{3+}. To avoid ambiguity, such as in cases where XRF data is reported as Fe_2O_3, but the speciation is unknown compared to situations when the proportions of FeO and Fe_2O_3 are known, total FeO contents should be used in input spreadsheets for all phases (labelled "FeOt_Liq", "FeOt_Cpx" etc.). To partition melt Fe between redox states, the input spreadsheet may contain a column labelled "Fe3Fet_Liq" specifying the decimal fraction of Fe^{3+} in the liquid. None of the models considered here are sensitive to user-entered Fe redox proportions in phases other than liquid.

By default, functions involving liquid compositions use the value of `Fe3Fet_Liq` in the input spreadsheet, which is 0 if no column heading with this name is provided. `Fe3Fet_Liq` can also be overwritten in each function itself by specifying a fixed value (or referencing a different column in the input spreadsheet, e.g., `Fe3Fet_Liq=0.4`, or `Fe3Fet_Liq=df['column_name']`).

Alternatively, the function `convert_fo2_to_fe_partition` in Thermobar calculates the Fe^{3+}/Fe_T ratio and partitions iron between FeO and Fe_2O_3 for user-supplied liquid compositions at a given pressure and temperature, and specified oxygen fugacity (fo_2 value, or buffer position in terms of ΔQFM or ΔNNO). This means users can first convert a fo_2 value or buffer into a Fe^{3+}/Fe_T ratio for each sample, and use this to perform calculations, rather than using a fixed Fe^{3+}/Fe_T ratio.

3.6 Data Outputs

Thermobar returns two main types of outputs. For simple calculations, such as calculating temperature for a given melt composition and pressure, it returns a pandas series (a single column of data). For more complicated calculations with more than one output (e.g., pressure and temperature for iterative calculations, or when a user specifies they

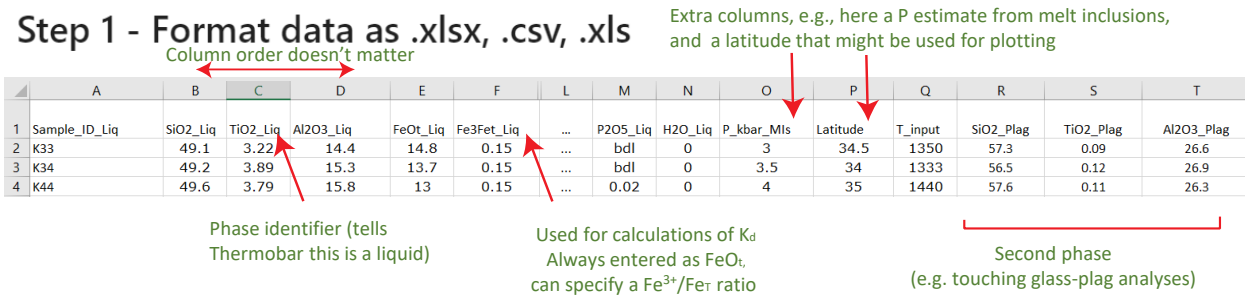

	A	B	C	D	E	F	L	M	N	O	P	Q	R	S	T
1	Sample_ID_Liq	SiO2_Liq	TiO2_Liq	Al2O3_Liq	FeOt_Liq	Fe3Fet_Liq	...	P2O5_Liq	H2O_Liq	P_kbar_MIs	Latitude	T_input	SiO2_Plag	TiO2_Plag	Al2O3_Plag
2	K33	49.1	3.22	14.4	14.8	0.15	...	bdl	0	3	34.5	1350	57.3	0.09	26.6
3	K34	49.2	3.89	15.3	13.7	0.15	...	bdl	0	3.5	34	1333	56.5	0.12	26.9
4	K44	49.6	3.79	15.8	13	0.15	...	0.02	0	4	35	1440	57.6	0.11	26.3

Step 2 - Import required python packages and Thermobar

```
# This installs Thermobar, it only needs to be run once.
!pip install Thermobar
```

```
import Thermobar as pt              # Imports Thermobar after a user has run "!pip install Thermobar"
import numpy as np                  # Imports numpy, used for various math operations.
import pandas as pd                 # Imports pandas, used for data manipulation and display
import matplotlib.pyplot as plt     # Imports matplotlib, used for plotting
```

Step 3 - Import data from a specific Excel Sheet

```
#This line reads in columns from Sheet1 of the spreadsheet.
#It returns a dictionary (collection of dataframes) which we have named "out"
out=pt.import_excel('Example_Excel_input.xlsx', sheet_name="Sheet1")
my_input=out['my_input']
myLiquids=out['Liqs']    # This extracts the dataframe of Liq compositions
myPlags=out['Plags']     # This extracts the dataframe of Plag compositions
myOls=out['Ols']         # This dataframe will be full of zeros, as no olivine compositions were provided
```

Step 4 - Inspect the data to ensure it read correctly

```
display(myLiquids.head()) # Prints the first 5 rows of myLiquids
display(myPlags.head())   # Prints the first 5 rows of myPlags
```

	SiO2_Liq	TiO2_Liq	Al2O3_Liq	FeOt_Liq	MnO_Liq	MgO_Liq	CaO_Liq	Na2O_Liq	K2O_Liq	Cr2O3_Liq	P2O5_Liq	H2O_Liq	Fe3FeT_Liq	NiO_Liq	CoO_Liq	CO2_Liq	Sample_ID_Liq
0	49.1	3.22	14.4	14.8	3.20	3.20	6.72	3.34	1.70	0.0	0.00	0	0.15	0.0	0.0	0.0	K33
1	49.2	3.89	15.3	13.7	3.88	3.88	6.76	3.44	1.22	0.0	0.00	0	0.15	0.0	0.0	0.0	K34
2	49.6	3.79	15.8	13.0	4.26	4.26	6.59	3.65	1.04	0.0	0.02	0	0.15	0.0	0.0	0.0	K44

	SiO2_Plag	TiO2_Plag	Al2O3_Plag	FeOt_Plag	MnO_Plag	MgO_Plag	CaO_Plag	Na2O_Plag	K2O_Plag	Cr2O3_Plag	Sample_ID_Plag
0	57.3	0.09	26.6	0.43	0	0.03	8.33	6.11	0.49	0	0
1	56.5	0.12	26.9	0.47	0	0.05	8.95	5.66	0.47	0	1
2	57.6	0.11	26.3	0.50	0	0.07	8.50	6.27	0.40	0	2

Fills missing columns with zeros

Figure 3: Guide to data input. **Step 1**: Format data into a spreadsheet with oxide names followed by _phase. The order of columns doesn't matter, and other columns can also be included in the input (e.g., estimates of pressure and temperature, additional sample information etc). **Step 2**: Thermobar is imported, along with numpy, pandas and matplotlib. **Step 3**: The `import_excel` function extracts data from this spreadsheet into a set of dataframes with specific a specific column order. The function returns a dictionary (named "out") where all these dataframes are stored with keys corresponding to different phases. For example, the dataframe of liquids is extracted from this dictionary using the key "Liqs". All dictionary keys correspond to the phase identifiers used for inputs with an added "s". If the input doesn't have specific column headings (e.g., no _Ol, _Kspar), the dataframe for this phase will be filled with zeros. **Step 4**. Dataframes for each phase are inspected to check that the spreadsheet has been read in correctly.

want equilibrium parameters to be evaluated), it returns a pandas dataframe (df). Any single column of a dataframe can be accessed by specifying the column name in square brackets after the name of the dataframe: `df['column_name']`.

At any point, the outputs of Thermobar can be written to an Excel spreadsheet using the pandas `to_excel` function. An example of this is provided in the Liquid-only thermometry section below.

3.7 Warnings

Thermobar contains a number of warnings from the papers of various thermobarometers, which should help to direct users when they are using a model outside its calibration range. These are far from exhaustive, because they rely on the original authors specifying reasonable calibration limits. For example, if users enter any liquid compositions with SiO_2>68 wt%, and select the Cpx-Liq barometer of Neave and Putirka [2017], the code will return the message "Some inputted liquids have SiO2>68 wt%, which exceeds the upper calibration range of the Neave and Putirka (2017) model" (see Fig. 6).

3.8 Calibration Ranges

In addition to pre-programmed warnings, the function `generic_cali_plot` can be used to generate a plot showing user-entered mineral or glass data alongside the calibration dataset of different thermobarometry models in P-T-X space (for models where the dataset was published or obtained by the authors; e.g. Ridolfi [2021], Putirka [2016], and Mutch et al. [2016] for Amp, Putirka [2008], Masotta et al. [2013], Neave and Putirka [2017], Brugman and Till [2019], Petrelli [2021], Jorgenson et al. [2021] and Wang et al. [2021] for Cpx, Waters and Lange [2015] and Masotta and Mollo [2019] for Plag).

For example, to generate a plot showing Al_2O_3 vs. Mg# of the user-entered amphibole compositions stored in the dataframe "Amps1" alongside the calibration data of Mutch et al. [2016]:

```
pt.generic_cali_plot(df=Amps1,
model="Mutch2016", x='Mgno_FeT',
y='Al2O3_Amp')
```

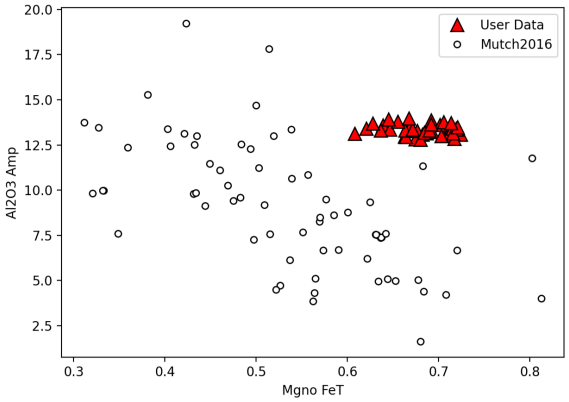

The order of the user data vs. calibration data can be adjusted, along with symbol size, color, transparency etc in this custom function. Alternatively, the calibration dataset can be obtained as a pandas dataframe allowing users to make their own plots in matplotlib:

```
pt.return_cali_dataset(model="Mutch2016")
```

3.9 Worked Examples

In this manuscript, we show a number of examples using snippets of code. Entire workflows can be found on the Read The Docs html webpage (https://thermobar.readthedocs.io), with narrated examples on the Thermobar YouTube channel (https://www.youtube.com/channel/UC7ddceuNnikCdQa_fRHmdXw). The Jupyter Notebooks and associated Excel files for these worked examples can be downloaded directly from the Read The Docs page, or from the Thermobar Github page (https://github.com/PennyWieser/Thermobar/tree/main/docs/Examples). Examples exist for the following workflows, and we are happy to add additional examples in future:

Liquid and Olivine-Liquid Equilibra

- Calculating temperature and water contents from liquid compositions and olivine-liquid pairs.
- Calculating equilibrium olivine forsterite contents from a specific melt composition using a variety of $K_{D,Fe-Mg}$ models.
- Plotting Ol-Liq pairs on Rhodes diagram (Liq Mg# vs. Ol Fo), with lines for different equilibrium models.

Cpx and Cpx-Liq Equilibra

- Calculating P for known T, T for known P, and iteratively solving P and T for Cpx-only and Cpx-Liq pairs, including assessment of various equilibrium tests.

- Plotting Cpx-Liq pairs on a Rhodes diagram (Liq Mg# vs. mineral Mg#).
- Plotting Cpx compositions on a ternary classification diagram (En-Fs-Wo).
- Cpx-Liq melt matching recreating the studies of Scruggs and Putirka [2018] and Gleeson et al. [2020].

Opx and Opx-Liquid Equilibra

- Calculating P for known T, T for known P, iteratively solving P and T for Opx-only and Opx-Liq pairs, including assessment of $K_{D,Fe-Mg}$ equilibrium.
- Plotting Opx-Liq pairs on a Rhodes diagram.
- Plotting Opx compositions on a ternary diagram (En-Fs-Wo).
- Assessing all possible Opx-Liq pairs filtered by $K_{D,Fe-Mg}$.

Two Pyroxene Equilibra

- Calculating P for known T, P for known T, iteratively solving P and T, assessment of $K_{D,Fe-Mg}$ equilibrium.
- Assessing all possible Opx-Cpx matches filtered by $K_{D,Fe-Mg}$.

Amp and Amp-Liq Equilibra

- Calculating P for known T, T for known P, iteratively solving P and T for Amp-only and Amp-Liquid pairs, including assessment of $K_{D,Fe-Mg}$ equilibrium.
- Calculating melt compositions, water contents and redox states from Amp compositions using Putirka [2016] and Zhang et al. [2017].
- Assessing all possible Amp-Liq matches filtered by $K_{D,Fe-Mg}$.
- Plotting Amp compositions on classification diagrams following Leake et al. [1997].

Fspar and Fspar-Liq Equilibra

- Calculating T for known P and equilibrium tests for Plag-Liq, Kspar-Liq, and Plag-Kspar equilibria.
- Calculating H_2O using various Plag-Liq hygrometers, including iterating temperature and H_2O towards a solution.
- Iteratively solving P and T for Plag-Liq.
- Assessing all possible Plag-Liq, Kspar-Liq and Plag-Kspar matches filtered by various equilibrium tests proposed by Putirka [2008].
- Plotting Plag and Kspar compositions on a ternary diagram (An-Ab-Or).

Garnet and geotherm calculations

- Calculating T, and P for known T using garnet compositions.
- Plotting garnet geotherms and garnet compositional sections.

Error Propagation

- Propagating analytical errors for Liq-only thermometry, Cpx-Liq, and Cpx-only barometry.

Melt Inclusion Equilibrium

- Integrating Thermobar with VESIcal (Iacovino et al. [2021]) to iteratively calculate saturation pressure from melt inclusions with temperatures from melt or mineral-melt thermometry.
- Assessing Fe-Mg equilibration between melt inclusions and host olivines, and host olivines and co-erupted matrix glass.

Other Functions

- Plotting mineral and glass data with the calibration dataset of different models in P-T-X space.
- Converting between Fe^{3+}/Fe_T, fO_2 and buffer position.
- Calculating viscosity using the model of Giordano et al. [2008].
- Converting from oxide wt% to element wt% without and without oxygen.
- Converting pressures to depths using a variety of crustal density models.

4 Mineral-Melt Component Calculations

The underlying functions used for a wide range of different thermobarometers, hygrometers and chemometers calculate mole and cation proportions and fractions for each mineral (stored within the core.py file). For example, the function `calculate_anhydrous_mol_proportions_liquid` calculates the anhydrous mole proportions for user-specified liquid compositions, while `calculate_hydrous_cat_fractions_liquid` calculates cation fractions on a hydrous basis. Similarly, `calculate_6oxygens_orthopyroxene` calculates cations on the basis of 6 oxygens for Opx compositions, and `calculate_23oxygens_amphibole` calculates cations on the basis of 23 oxygens for

Amp compositions. More advanced functions such as `calculate_clinopyroxene_liquid_components` calculates mole and cation fractions for Liq and Cpx compositions, as well as various Cpx-Liq components. These core functions can be used when investigating natural mineral and melt compositions, as well as when producing new thermobarometers, and performing other calculations in petrology requiring these variables.

5 Useful Petrographic plots

To aid with visualization of mineral compositions, and the degree of mineral-melt equilibrium, we also include a number of functions for plotting of imported mineral data on common classification diagrams. For example, the function `calculate_ol_rhodes_diagram_lines` calculates the equilibrium lines for an olivine-liquid equilibrium "Rhodes Diagram". Together with the functions `calculate_liq_mgno` and `calculate_ol_fo` this allows users to easily plot olivines from different eruptions against the co-erupted glass Mg#, with equilibrium fields of their choosing overlain (Fig. 4a). These functions could also be applied to whole-rock data (also loaded with `_Liq` suffixes instead of glass data to assess olivine-whole rock relationships, such as olivine accumulation). The function `tern_points_px` takes imported pyroxene compositions and calculates the coordinates in En-Wo-Fs space, while the function `plot_px_classification` draws the plot and fields on which to overlay these new coordinates (Fig. 4b). Similarly, `tern_points_fspar` calculates ternary coordinates in An-Ab-Or space, and `plot_fspar_classification` draws the composition fields from Deer et al. [1992] on the figure (Fig. 4c). Example Jupyter notebooks show how to produce these plots in detail can be found on the Read The Docs page under the section for each mineral.

6 Single-phase thermobarometers and chemometers

Thermobar contains a number of thermometers and barometers based on the composition of a single phase:

- Liq-only thermometry
- Cpx-only thermometry and barometry
- Opx-only barometry
- Amp-only thermometry, and barometry and chemometry
- Gt-only thermometry and barometry

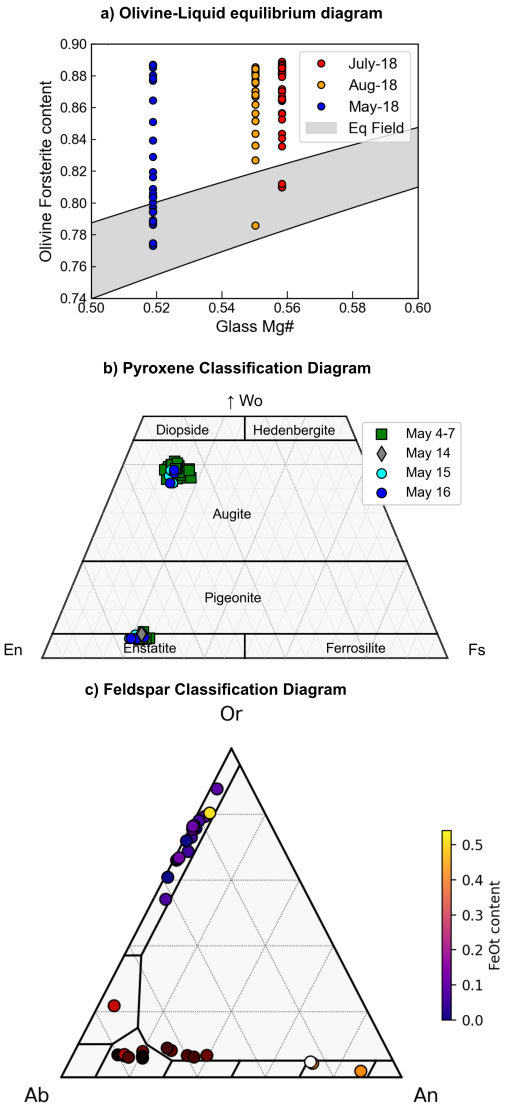

Figure 4: Example plots produced in Thermobar. a) Olivine-Liquid Equilibrium diagram for samples erupted in May, July and Aug during the 2018 eruption of Kīlauea Volcano from Wieser et al. [2021]. The equilbrium field spans K_D values of 0.27-0.354 (lower bound from Roeder and Emslie [1970], upper bound from Matzen et al. [2011]). b) Pyroxene classification, with Opx and Cpx compositions from the 2018 eruption of Kīlauea from Wieser et al. [2022] overlain, with symbols and colors representing different phases of the eruption defined by their date. c) Co-existing Plag and Kspar compositions from the experiments of Elkins and Grove [1990]. Symbols are colored based on the FeO_t content of each feldspar.

We discuss some examples for liquid-only thermometry, but the flexibility of function inputs is the same for other single-phase thermobarometers.

6.1 Liquid-only thermometers

Liquid-only thermometers vary widely in complexity. For example, the thermometer of Helz and Thornber [1987] calculates the temperature of a liquid (i.e. melt) based solely on the MgO content, while equation 15 of Putirka [2008] uses the MgO, FeO, Na_2O, K_2O, H_2O content and Mg# of the liquid, as well as an estimate of the pressure. For liquid-only thermometers, most equations calculate the temperature of the liquid, but equations in Thermobar with names ending with "_sat" calculate the temperature at which a liquid is saturated in a specific phase (Fig. 8). For example, equation 34 of Putirka [2008] calculates the temperature at which Cpx would saturate in the liquid (termed the saturation surface). Unless the phase has just appeared on the liquidus, these saturation temperatures are likely higher than the temperature of the liquid from which the mineral phase grew.

Several liquid-only themometers are adapted from olivine-liquid thermometers, where the D_{Mg} term that would traditionally be calculated from the partitioning of Mg between measured olivine-liquid pairs is replaced with a theoretical value of D_{Mg}, calculated from the liquid composition using the model of Beattie [1993]. These equations are indicated with _BeattDMg in their name, and are particularly useful because many olivine crystals are not in Fe-Mg equilibrium with their co-erupted carrier melts (see section *7.0.2*), so it is difficult to select an olivine and liquid composition in equilibrium.

Liquid-only thermometery calculations are performed using the function `calculate_liq_only_temp`. The required inputs are a dataframe of liquid compositions, as well as specifying `equationT = " "`. For example, for a pandas dataframe of liquids named "myLiquids" as in Fig. 3, temperature using the MgO thermometer of Helz and Thornber [1987] would be calculated as follows:

```
Temp_HT87=pt.calculate_liq_only_temp(
liq_comps=myLiquids,  equationT="T_Helz1987_MgO")
```

If equation 15 of Putirka [2008] is selected, Thermobar returns an error because this equation is P-sensitive:

```
Temp_eq15=pt.calculate_liq_only_temp(
liq_comps=myLiquids, equationT="T_Put2008_eq15")
```

```
Exception: You've selected a P-dependent function,
please pass an option for P (see help for more detail)
```

There are a number of ways to specify pressure. Firstly, a constant value of pressure can be specified for all liquids (here, P=5 kbar):

```
Temp_eq15_5kbar=pt.calculate_liq_only_temp(
liq_comps=myLiquids, equationT="T_Put2008_eq15",
P=5)
```

Alternatively, if the input spreadsheet contains a column for P in kbar (labelled "P_input") with different values for different liquids, P can be set to equal the values in this column by referencing the dataframe containing all columns (named my_input) returned from the `import_excel` function (See Fig. 3), and the column name in square brackets:

```
Temp_eq15_Pin=pt.calculate_liq_only_temp(
liq_comps=myLiquids, equationT="T_Put2008_eq15",
P=my_input['P_input'])
```

If pressure isn't known, setting `P="Solve"` will return a partial function:

```
Partial_eq15=pt.calculate_liq_only_temp(
liq_comps=myLiquids, equationT="T_Put2008_eq15",
P="Solve")
```

This can then be evaluated at any particular P by typing the name of this partial function and the pressure in kbar in brackets:

```
P_eq15_3kbar=Partial_eq15(3)
```

For large numbers of calculations this is more efficient than running the function again and again at a different pressure, because cation fractions, and other P-insensitive calculation steps are already evaluated in this partial function, so don't need to be re-evaluated when the pressure is changed.

Some liquid-only thermometers are also sensitive to melt H_2O content (see Fig. 8), which is often poorly constrained in volcanic systems with no rapidly quenched tephra suitable for melt inclusion analyses. By default, Thermobar will read H_2O contents from the `H20_Liq` column of the input spreadsheet. If the input spreadsheet has no column for H_2O, this column is filled with zeros. Input water contents can be overwritten when calling the function by specifying `H20_Liq=...`, allowing an easy way to investigate the effect of uncertain H_2O contents on temperatures. For example, here we evaluate temperatures at 6 wt% H_2O:

```
Temp_eq15_6H=pt.calculate_liq_only_temp(
liq_comps=myLiquids, equationT="T_Put2008_eq15",
P=5, H20_Liq=6)
```

As for pressure, H_2O can also be set to the value of any column in the input spreadsheet using `H20_Liq=my_input['column name']`. E.g. to use H_2O contents measured by Raman spectroscopy stored in a column labelled H2O_Raman:

```
Temp_eq15_Hin=pt.calculate_liq_only_temp(
liq_comps=myLiquids, equationT="T_Put2008_eq15",
P=5, H2O_Liq=my_input['H2O_Raman'])
```

6.1.1 *Saving to Excel*

Once calculations have been performed in Thermobar, there are a number of ways to save calculations to an Excel workbook to interact with them outside of Python. To save the temperatures alongside the liquid compositions, it is easiest to first make a copy of the original dataframe using the .copy() function. This means that the original is still preserved in the script for further calculations and previous results are not accidentally overwritten:

```
Liq_T_out=myLiquids.copy()
```

Then, the pandas series generated by each calculation can be added onto this dataframe using the pandas .insert() function. Users need to specify a number for which position they want this new column in (loc), the name of the column (column) and the variable they wish to save in that column (value).

```
Liq_T_out.insert(loc=0, column="Temp HT87",
value=Temp_HT87)
Liq_T_out.insert(loc=1, column="Temp eq15 5kbar",
value=Temp_eq15_5kbar)
Liq_T_out.insert(loc=2, column="Temp eq15 Pin",
value=Temp_eq15_Pin)
```

Here, we saved the calculations from Helz and Thornber [1987] to the 1st column of the dataframe (python numbering starts from zero), and calculations from Putirka [2008] equation 15 at 5 kbar to the second column, and calculations using pressure from the P input column to the third column respectively. Finally, this new dataframe can be saved to an Excel spreadsheet (here named "Liquid_only.xlsx"):

```
Liq_T_out.to_excel('Liquid_only.xlsx')
```

Further examples of saving various data structures to Excel can be found at Read The Docs.

6.2 Mineral-only thermometers and barometers

Mineral-only thermometers and barometers are implemented in a very similar way to liquid thermometers. For example, to calculate amphibole-only pressures using the barometer of Mutch et al. [2016]:

```
pt.calculate_amp_only_press(
amp_comps=myAmps, equationP="P_Mutch2016")
```

Where myAmps is dataframe of amphibole compositions from the `import_excel` function.

Similarly, to calculate Cpx-only pressure using the temperature-dependent barometer given by equation 32b of Putirka (2008):

```
pt.calculate_cpx_only_press(cpx_comps=myCpxs,
equationP="P_Put2008_eq32b", T=1400)
```

Where myCpxs is dataframe of Cpx compositions from the `import_excel` function, and 1400 is the temperature in Kelvin at which to perform calculations.

6.3 Iterative calculations

Unlike for experimental studies, in natural systems it is likely that neither temperature or pressure is known. To address this, Thermobar contains functions to iterate towards a solution using an equation for pressure and an equation for temperature. The names of these function are adapted from those discussed above by adding the ending _press_temp (e.g., `calculate_cpx_only_press_temp`).

By default, these functions start with T=1300 K, which is input into the selected barometer to calculate a pressure. This calculated pressure is then entered into the selected thermometer, and this process is repeated for 30 iterations. If necessary, users can overwrite both the initial T and number of iterations, although in a multitude of tests, this method converged on a solution identical to the Excel iteration used in the spreadsheets of K. Putirka, and reduces the computational cost of the function.

For example, the following code calculates both pressure and temperature using only cpx compositions, and the thermometer of Putirka (2008) eq32d for temperature and equation 32a for pressure:

```
pt.calculate_cpx_only_press_temp(cpx_comps=myCpxs,
equationP="P_Put2008_eq32a",
equationT="T_Put2008_eq32d")
```

This returns a pandas dataframe, with columns for calculated pressure and temperature:

	P_kbar_calc	T_K_calc
0	5.330423	1487.588565
1	4.912641	1476.307186
2	5.904306	1501.021450

6.4 Mineral-only Chemometers

At present, only Amp-only chemometers are implemented in Thermobar. To calculate co-existing equilibrium liquid compositions using Zhang et al. [2017] for SiO_2, TiO_2, FeO, MgO, CaO, K_2O, Al_2O_3, and calculated H_2O contents, ΔNNO values from Ridolfi [2021] for a dataframe of amphibole compositions called myAmps:

```
pt.calculate_amp_only_melt_comps(amp_comps=myAmps)
```

K2O_Eq12_Zhang17	K2O_Eq13_Zhang17	Al2O3_Eq14_Zhang17	H2O_Ridolfi21	deltaNNO_Ridolfi21
2.378780	2.334718	17.886312	6.221705	2.781062
1.974113	2.730521	17.962779	9.282463	1.956064
2.916734	2.438641	17.480366	4.148120	2.869497
3.330558	2.619149	16.370036	4.303575	2.046019
2.908677	2.620235	16.658488	5.642425	1.799559

As well as a dataframe of results, this function also returns a warning, stating: "You must enter a value for T in Kelvin to get results from equation3 and 5 from Zhang, and SiO2 from Putirka (2016)". These additional equations are evaluated when a temperature is specified within the function:

```
pt.calculate_amp_only_melt_comps(
amp_comps=myAmps, T=1300)
```

In many cases, the temperature may not be known. Thus, the user could first calculate Amp-only pressure and temperature by iterating the barometer of Ridolfi [2021] with the thermometer of Ridolfi and Renzulli [2012]:

```
PT_Rid=pt.calculate_amp_only_press_temp(
amp_comps=myAmps,
equationP="P_Ridolfi2021",
equationT="T_Ridolfi2012",
Ridolfi_Filter=True)
```

By default, Amp compositions failing the various filters of Ridolfi (2021) return NaNs for P and T. You could specify `Ridolfi_Filter=False` such that numbers are still returned for P and T (although users should inspect the column "Fail Msg" in the dataframe `PT_Rid` to see which ones failed and why, such as low totals, not Mg-hornblendes etc.). Then, the calculated temperature from this dataframe (named PT_Rid, column name `T_K_Calc`) can be fed into the chemometry function:

```
pt.calculate_amp_only_melt_comps(
amp_comps=myAmps, T=PT_Rid['T_K_calc'])
```

7 Two-phase thermometers and barometers

The following thermometers, barometers and hygrometers are based on equilibrium between two phases. The application of these functions generally requires more thought from the user. In an ideal scenario, calculations are performed on phases which have a clear textural relationship, such as measurements of spinels trapped within a specific olivine crystal (Matthews et al. [2016]), or measurements of touching Cpx-Opx pairs (Walker et al. [2013]). However, in many natural samples, this is simply not possible. For example, disaggregation of crystals during transport and eruption mean that it is very common that erupted lavas and tephra samples have few, or no touching pairs of crystals. Even if crystals are touching, there is no guarantee that they are in chemical equilibrium, as crystals with different histories can be aggregated into clusters by flow within volcanic conduits and/or crystal settling (Wieser et al. [2019b], Culha et al. [2020]).

Thermobarometers which rely on the equilibrium between a liquid and crystal phase (rather than 2 crystal phases) are particularly problematic. Generally, only a narrow range of liquid composition will be erupted in any given phase of an eruption, while the erupted crystal cargo may be chemically diverse, having grown from a range of melt compositions undergoing chemical differentiation at depth. In many volcanic centers, the lack of glassy groundmass means it is difficult to even characterize the composition of this single "carrier liquid" bringing the crystals to the surface, as bulk analyses techniques such as XRF are sensitive to crystal addition. These pitfalls mean that it is very difficult to identify meaningful mineral-melt pairs in many volcanic systems.

In Thermobar, we provide a number of functions implementing workflows proposed in the literature for these less-than-optimal (but common) scenarios. We present algorithms which consider all possible matches between measured phases (e.g., assessing all possible liquid and pyroxene pairs, or all possible pairs of orthopyroxenes and clinopyroxenes), with user-defined equilibrium filters. Where relevant, the equilibrium tests available for each thermobarometer are discussed below.

7.0.1 *Olivine-Spinel Thermometry*

Thermobar includes the olivine-spinel thermometers of Wan et al. [2008] and Coogan et al. [2014] (Fig. 9), which are both pressure-independent. The input spreadsheet should be prepared such that each row contains an olivine compositions (column headings: SiO2_Ol, MgO_Ol...) and a spinel composition (SiO2_Sp..., MgO_Sp). After using the `import_excel` function, these thermometers are called using the function `calculate_ol_sp_temp`:

```
pt.calculate_ol_sp_temp(
liq_comps=myLiquids, sp_comps=mySps,
equationT="T_Wan2008")
```

Where myOls is a dataframe of olivine compositions, mySps is a dataframe of spinel compositions, and the thermometer is from Wan et al. [2008].

To our knowledge, there are no available Ol-Sp equilibrium tests, although the fact that spinels are often incorporated within olivines, along with the slow diffusion rate of Al, means disequilibrium is unlikely to be an issue.

7.0.2 *Olivine-Liquid Thermometry*

As with olivine-spinel thermometry, the default way to calculate olivine-liquid temperatures in Thermobar is to prepare an Excel spreadsheet with each row containing an olivine composition paired with a specific liquid composition. For all olivine-liquid thermometers except that of Pu et al. [2017], a pressure needs to be specified (as in section 7.0.2). For example, temperatures can be calculated using equation 21 of Putirka [2008] at 5 kbar:

```
pt.calculate_ol_liq_temp(
liq_comps=myLiquids, ol_comps=myOls,
equationT="T_Put2008_eq21", P=5)
```

This function returns a pandas dataframe with the temperature in Kelvin as well as the measured $K_{D,\ Fe\text{–}Mg}^{Ol\text{–}Liq}$.

Unlike olivine-spinel thermometry, olivine-liquid thermometry is highly susceptible to issues involving disequilibrium. This is because olivine crystals are commonly "antecrystic", being brought to the surface in chemically-unrelated melts (Wieser et al. [2019a]; Balta et al. [2013]). Thus, it is vital to calculate the degree of equilibrium for olivine-liquid pairs to assess the accuracy of thermometric estimates. The most common way to assess olivine-melt equilibrium examines the partition coefficient of Fe-Mg between these two phases ($K_{D,\ Fe\text{–}Mg}^{Ol\text{–}Liq}$, returned by default for Ol-Liq functions). The value of $K_{D,\ Fe\text{–}Mg}$ is sensitive to redox. By default, all Thermobar functions use the value of `Fe3Fet_Liq` in the user input, and Ol-Liq K_D is calculated using only Fe^{2+} in the liquid phase. The proportion of Fe^{3+} used in the calculation can be overwritten by specifying a different value for `Fe3Fet_Liq`. Here we perform calculations using 20% Fe^{3+}:

```
pt.calculate_ol_liq_temp(
liq_comps=myLiquids, ol_comps=myOls,
equationT="T_Put2008_eq21", P=5,
Fe3Fet_Liq=0.2)
```

If `eq_tests=True` is specified in the function, equilibrium K_D values are calculated from the liquid composition using the models of Toplis [2005], Matzen et al. [2011] and Roeder and Emslie [1970]:

```
pt.calculate_ol_liq_temp(
liq_comps=myLiquids, ol_comps=myOls,
equationT="T_Put2008_eq21", P=5,
eq_tests=True)
```

As well as the calculated temperature, the measured K_D, and the calculated K_D for each model, and the input liquid composition, the function returns the difference between measured and calculated K_D values for these three models (all as a pandas dataframe):

	T_K_calc	Kd Meas	Kd calc (Toplis)	ΔKd, Toplis	ΔKd, Roeder	ΔKd, Matzen	SiO2_Liq
0	1306.09	0.31	0.33	0.02	0.01	0.02	57.02
1	1240.35	0.18	0.31	0.14	0.12	0.15	57.66
2	1286.37	0.27	0.32	0.05	0.03	0.06	60.73

In many cases, none of the pre-matched olivines and liquids will be in equilibrium. To help users determine the composition of olivines that would be in equilibrium with their liquids, the function `calculate_eq_ol_content` calculates the equilibrium olivine forsterite content for a given set of liquid compositions. As for the equilibrium test above, three models for predicting $K_{D,\ Fe\text{–}Mg}^{Ol\text{–}Liq}$ equilibrium are included. Specifying `Kd_model="Roeder1970"` uses $K_{D,\ Fe\text{–}Mg}$ =0.3±0.03 following Roeder and Emslie [1970], `Kd_model="Matzen2011"` uses $K_{D,\ Fe\text{–}Mg}$ =0.34±0.012 following Matzen et al. [2011].

For example, to calculate the equilibrium olivine content using the model of Roeder and Emslie [1970]:

```
pt.calculate_eq_ol_content(liq_comps=myLiquids,
Kd_model="Roeder_1970")
```

The pandas dataframe returned by the function has column headings corresponding to the equilibrium forsterite content for $K_{D,\ Fe\text{–}Mg}$=0.3 (preferred value), 0.33 (+1σ), and 0.27 (-1σ):

	Eq Fo (Roeder, Kd=0.3)	Eq Fo (Roeder, Kd=0.33)	Eq Fo (Roeder, Kd=0.27)
0	0.616254	0.593479	0.640846
1	0.677781	0.656623	0.700347
2	0.708781	0.688724	0.730041

Unlike the fixed $K_{D,\ Fe\text{–}Mg}$ values of Roeder and Emslie [1970] and Matzen et al. [2011], the model of Toplis [2005] calculates $K_{D,\ Fe\text{–}Mg}$ as a function of liquid composition, pressure, temperature, and olivine forsterite content. Thermobar provides several ways to use this model. First, using paired olivine and liquid compositions:

```
pt.calculate_eq_ol_content(
liq_comps=myLiquids, ol_comps=myOls,
Kd_model="Toplis2005", P=2, T=1373.1)
```

Alternatively, just the olivine forsterite content can be input as a single value or a pandas series (instead of the full olivine compositions), along with pressure, temperature, and liquid compositions:

```
pt.calculate_eq_ol_content(
liq_comps=myLiquids, ol_fo=0.82,
Kd_model="Toplis2005", P=2, T=1373.1)
```

In both cases, the function returns a pandas dataframe where the first column is the equilibrium $K_{D,\ Fe\text{–}Mg}$ calculated using Toplis [2005], and the second column is the equilibrium olivine

forsterite content. However, needing to specify an olivine forsterite content to calculate an equilibrium forsterite content is somewhat circular logic. If olivine compositions or a forsterite content are not entered into the function, Thermobar will iterate by first calculating a $K_{D,\ Fe-Mg}$ for Fo=0.95, then use this $K_{D,\ Fe-Mg}$ to calculate an equilibrium Fo content, and then inputting that Fo content into a new calculation for $K_{D,\ Fe-Mg}$ (over 20 iterations):

```
pt.calculate_eq_ol_content(
liq_comps=myLiquids, Kd_model="Toplis2005",
P=2, T=1373.1)
```

If `Kd_model="All"`, calculations are performed using all 3 models (including using the iterative approach for Toplis):

```
pt.calculate_eq_ol_content(
liq_comps=myLiquids, ol_comps=myOls,
Kd_model="All", P=2, T=1373.1)
```

7.1 Clinopyroxene-Liquid Thermobarometry

Thermobar contains a number of different thermometers/barometers applicable to Cpx-Liq pairs (Fig. 10). In simplest scenario where relevant Cpx-Liq pairs have been identified (e.g., experimental products, groundmass-rim pairs), data should be prepared as an Excel spreadsheet where each row contains a matched pair of Liq and Cpx compositions. The function `calculate_cpx_liq_press` allows users to calculate pressures for a variety of barometers, while the function `calculate_cpx_liq_temp` calculates temperature. For thermometers which are P-sensitive a pressure in kbar must be specified, and a temperature in K must be specified for T-sensitive barometers (as for the single-phase thermobarometers discussed above). For example, to calculate temperature using equation 33 of Putirka [2008] at 5 kbar:

```
pt.calculate_cpx_liq_temp(
liq_comps=myLiquids, cpx_comps=myCpxs,
equationT="T_Put2008_eq33", P=5)
```

When neither pressure or temperature is known, the function `calculate_cpx_liq_press_temp` iterates towards a solution using a user-supplied pressure and temperature by specifying an equation for both pressure and temperature. For example, here we iterate equation 33 for T and equation 30 for P from Putirka [2008]:

```
pt.calculate_cpx_liq_press(
liq_comps=myLiquids, cpx_comps=myCpxs,
equationT="T_Put2008_eq33",
equationT="T_Put2008_eq30").
```

To return the values of different equilibrium tests (e.g., DiHd, EnFs, Neave et al. [2019]), users can specify an additional argument `eq_tests=True` in all Cpx-Liq functions.

7.1.1 *Machine Learning models*

Thermobar also contains implementations of the extra trees machine learning (ML) Cpx-only and Cpx-Liq thermometers and barometers of Petrelli et al. [2020] and Jorgenson et al. [2021]. Thermobar is distributed using the free service PyPI, so that users can install it using the simple `pip install` command. However, PyPI has a size limit of 100 MB per "release" of the project. Given that pickle (.pkl) or onnx (.onnx) files used to save pre-trained ML models tend to be 10s of MB each, it is not possible to distribute all these presaved models as well as the other Thermobar source code in a single package.

Thus, in addition to pip installing Thermobar once on their machine, users who wish to use machine learning models will need to run an additional line in their notebook specifying that they wish to download these saved models from the Github repository `Thermobar_onnx`:

```
!pip install "https://github.com/PennyWieser/Thermobar_onnx/archive/refs/tags/0.02.zip"
```

Once these files have been downloaded once, they can be accessed the same way as more conventional empirical thermobarometers:

```
pt.calculate_cpx_liq_press(
liq_comps=myLiquids, cpx_comps=myCpxs,
equationP="P_Petrelli2020_Cpx_Liq").
```

Following the work of Jorgenson et al. [2021], as well as returning the calculated pressure or temperature obtained from averaging across all decision trees (column `P_kbar_calc`), we also return the median, standard deviation, and interquartile range calculated from all the trees used:

	P_kbar_calc	Median_Trees	Std_Trees	IQR_Trees
0	6.781813	7.000	4.375027	7.300
1	10.679156	9.300	3.759244	5.000
2	8.477356	9.300	4.105941	4.985

This allows users to filter out rows which give very large interquartile ranges or standard deviations.

An ongoing problem with ML based thermobarometers is that even using the same code, different versions of scikit-learn will return different pressures and temperatures (with differences up to ~0.5 kbar). Additionally, ML models saved as pickles in one version of scikit-learn will yield a warn-

ing message when opened in a different version:

```
UserWarning: Trying to unpickle estimator StandardScaler from version 1.0.2 when using version 0.24.1. This might lead to breaking code or invalid results. Use at your own risk.

UserWarning: Trying to unpickle estimator ExtraTreeRegressor from version 1.0.2 when using version 0.24.1. This might lead to breaking code or invalid results. Use at your own risk
```

These warnings are not concerning in themselves because the answer obtained from one versions is not more correct than that from any other version, and differences are well within the stated SEE of the model. However, different results based on the specifics of the local python installation does represent a problem in terms of ensuring results are reproducible.

One solution is to use Onnx (ONNX-Runtime-developers [2021]) to save ML pipelines, which ensures stable results. However, as of yet, there is no way to build the voting of Jorgenson et al. [2021] into these pipelines. Thus, in Thermobar, we include 2 versions of ML models:

1. `equationP="P_Petrelli2020_Cpx_only"` will calculate Pressure using voting for Petrelli [2021] from a model saved as a pickle, but the exact pressure will change with future versions.

2. `equationP="P_Petrelli2020_Cpx_only_onnx"` will use onnx to give a stable answer, but can't currently do voting.

The same suffix format applies to the models from Jorgenson to access these two options

With time, we anticipate the pickles will eventually stop loading into newer version of scikit-learn. We will re-release new .pkl files (and .onnx files if required) when this happens, so users should check for the latest version number from https://github.com/PennyWieser/Thermobar_onnx/tags, and upgrade their installation:

```
pip install --upgrade  "GitHub-url-new-tag"
```

We will also update this repository to add new ML models as they emerge.

7.1.2 *Cpx-Liq Melt Matching*

A number of methods have been developed to perform Cpx-Liq thermometry by compared all erupted Cpx and Liq compositions from a given volcanic center/region, and identifying liquid-cpx pairs which meet certain equilibrium criteria (e.g., Neave and Putirka [2017], Neave et al. [2019], Winpenny and Maclennan [2011], Scruggs and Putirka [2018]). In Thermobar, the function `calculate_cpx_liq_press_temp_matching` assesses all possible clinopyroxene-liquid pairs for a user-supplied dataframe of liquid compositions of length N (e.g., all XRF analyses from a given volcanic center), and a user-supplied dataframe of measured Cpx compositions of length M. The function performs the following steps:

1. Liq components and Cpx components (e.g., cation fractions) are calculated for each individual sample (saving computational time vs. calculating them after the duplication steps below).

2. Each Cpx composition (oxides+components) is duplicated N times forming a pandas dataframe with rows for Cpx1-Cpx1-Cpx1, ..., CpxN-CpxN-CpxN. The dataframe of liquid compositions (raw+components) is duplicated M times forming a dataframe of the form Liq1-Liq2-Liq3...LiqM, Liq-Liq2-Liq3...LiqM, These dataframes are combined, creating a dataframe of length N*M with all possible Cpx-Liq pairings of the format Cpx1-Liq1, Cpx1-Liq2, Cpx1-Liq3, Cpx2-Liq1... CpxN-LiqM.

3. Compositional components which require both a Liq and Cpx composition are calculated for this combined dataframe (e.g., the DiHd component, $K_{D,\ Fe-Mg}^{Cpx-Liq}$).

Step 3 is complex. As Cpx-Liq equilibrium tests are sensitive to pressure and/or temperature, equilibrium tests cannot be performed until pressures and temperatures for each pair have been calculated. However, calculating pressures and temperatures iteratively for all possible Cpx-Liq matches can be very time consuming (e.g., 400 Cpx and 2500 possible liquids requires 1 million iterative calculations to be performed). To increase computational efficiency, we apply a preliminary filter in terms of $K_{D,\ Fe-Mg}$ equilibrium (using equation 35 of Putirka [2008] by default). As $K_{D,\ Fe-Mg}$ parametrizations are sensitive to temperature but not pressure, we use the `calculate_cpx_liq_temp` function to calculate a minimum temperature for each Cpx (for P=-10 bars), and a maximum temperature (for a default maximum pressure of 30 kbars). This upper pressure limit was set with volcanic systems in mind, but can be easily overridden when calling the function by setting `PMax=" "`. These maximum and minimum equilibrium $K_{D,\ Fe-Mg}^{Cpx-Liq}$ values are compared to the measured $K_{D,\ Fe-Mg}$ values for each Cpx-Liq pair. If the deviation between measured and calculated $K_{D,\ Fe-Mg}$ is greater the specified value (0.03 by default, changed by specifying `Kd_Err=" "`) for both the minimum and maximum equilibrium $K_{D,\ Fe-Mg}$, no temperatures in-between will yield a match. Thus, these Cpx-Liq matches can be discarded.

4. The function `calculate_cpx_liq_press_temp` is used to iteratively calculate pressures and temperatures for remaining Cpx-Liq pairs.

5. Using the calculated temperature and pressure for each pair, the equilibrium $K_{D,\ Fe-Mg}$ is calculated using equation 35 of Putirka [2008], the equilibrium CaTs component using the expression of Putirka [1999], and the updated equilibrium EnFs and DiHd components calculated using the expression of Mollo et al. [2013], following Neave et al. [2019]. Other models for these equilibrium tests can also be specified in the function. It is worth noting that the supplementary spreadsheet of Neave et al. [2019] uses the Putirka (1996) anhydrous thermometer to calculate the $K_{D,\ Fe-Mg}$ component, while temperature is calculated using equation 33. In our code, $K_{D,\ Fe-Mg}$ is calculated using the user-specified thermometer for consistency.

6. By default, Thermobar then selects Cpx-Liq pairs where the measured components calculated using the method of Putirka et al. [1996] and calculated equilibrium components are within ±0.03 for $K_{D,\ Fe-Mg}$, ±0.06 for DiHd, ±0.05 for EnFs, and ±0.03 for CaTs (following the supporting Excel spreadsheet of Neave et al. [2019]). Users can change these selection criteria using `DiHd_Err=...`, `Kd_Err=...` etc.

7. The function returns a dictionary. Users can extract a pandas dataframe of all Cpx-Liq matches which meet the specified equilibrium criteria using `dictionary_name['All_PTs']`. Following the approach of Neave and Putirka [2017], Thermobar also performs calculations to average the pressures and temperatures for each Cpx. For example, if Cpx1 matches with Liq1, Liq3, and Liq9, the values for these three matches will be averaged, and the standard deviation of the pressure and temperature are returned. This information is stored in the second part of the dictionary accessed using `dictionary_name['Av_PTs']`.

The speed at which these calculations are performed are significantly faster than previous tools (seconds vs. tens of minutes for assessing matches between hundreds of possible Cpx and Liqs). This, along with the flexibility provided by the implementation of these tools in python, offers users a lot more freedom to assess possible Cpx-Liq matches in larger datasets. There is also far more choice of equilibrium filters. For example, users can specify `Kd_Match="Masotta"`, which calculates $K_{D,\ Fe-Mg}$ using equation 35Alk of Masotta et al. [2013]. This equation expresses $K_{D,\ Fe-Mg}$ as a function of temperature, and the cation fractions of Na_2O and K_2O in the melt, and was developed for trachyte and phonolitic magmas (extreme care should be taken when applying it to other melt compositions). As with the other functions discussed so far, users can also specify `H2O_Liq` and `Fe3Fet_Liq` ratio in the function itself. This can be a fixed value for all calculations, or could be set as a pandas series with the same length as the input dataframe of liquid compositions.

7.1.3 *Recreating Scruggs and Putirka (2018)*

To demonstrate the versatility of this Cpx-Liq melt matching function, we recreate the analysis of Scruggs and Putirka [2018], who assess Cpx-Liq equilibrium on samples from Chaos Craggs at Lassen Peak. The erupted liquids sampled at Chaos Craggs are strongly bimodal. To capture the compositions of liquids which likely exist at depth between these two erupted end-members, Scruggs and Putirka [2018] add or subtract the composition of a felsic-whole rock composition from measured mafic liquids, and use the solver functions in Excel to find the mixing proportion that best satisfies equilibrium tests (https://www.youtube.com/watch?v=CjKvgXrah_k&list=PLnOXMT9X-AL_No_vUkkx8tYrahGQ1X4Kh&index=2&t=13s).

We demonstrate how a more automated approach can be implemented in Thermobar in Fig. 6 (this worked example is also available on the Read The Docs page). Step 1 imports an Excel spreadsheet containing possible liquid compositions (whole-rock data in this example), and a separate sheet or spreadsheet containing measured Cpx compositions (Fig. 5). Step 2 uses the function `add_noise_sample_1phase` to make a silicic end-member to use for mixing. We apply a filter to only consider measured liquids with > 65 wt% SiO_2, and for each measured liquid, we generate 5 duplicates, adding normally-distributed noise with 1σ=1% to all oxides. This helps to account for the fact that there are also a number of silicic liquids which exist at depth, but are not represented in sampling. We use the same function to make synthetic liquids based on the composition of measured samples with < 53.8 wt% SiO_2 and > 4 wt% MgO for the mafic end member. The following steps could also be performed using a dataframe of liquid compositions without any noise or filters added.

Step 3 mixes these end-members to generate synthetic liquids spanning the entire compositional range between measured liquids. The function `calculate_bootstrap_mixes` mixes these two end members in various proportions with a number of different options (demonstrated in the example notebook). In its simplest form, the function

takes two end members, and mixes a randomly-selected composition from one end member with a randomly-selected composition from the other end member, with the mixing proportion varying randomly between 0 and 1. Additional flexibility is provided by the optional input `self_mixing`. If `self_mixing=True`, the two end members are combined into a single dataframe, and these compositions are randomly mixed. This means that mixing happens: 1) between mafic and silicic end members (as in the default form) 2) between different mafic end member compositions, and 3) between different silicic end member compositoins. Self mixing produces a stronger clustering of synthetic liquids near the end members, which may be useful in certain circumstances. However, in this specific example, relatively few liquids generated by this function lie within the compositional gap between mafic and silicic compositions for <1000 duplicates. Thus, we use the option `self_mixing="Partial"`, which creates half the mixes by mixing between silicic and mafic end members, and the other half from self-mixing.

Step 4 is optional (Fig. 6), and combines this synthetic dataframe of liquids with the original dataframe of liquids using the pandas concat function (to include samples which weren't selected as end members).

Because Cpx thermometry is sensitive to the H_2O content of the liquid, but H_2O contents at depth cannot be deduced from bulk rock analyses of degassed lava samples, Scruggs and Putirka [2018] calculate the H_2O of the liquid as a function of the SiO_2 content. Step 5 overwrites the H_2O in the Liq dataframe (0 as whole-rock data) using their expression.

Step 6 inputs this finalized dataframe of synthetic and measured liquids, and measured Cpx compositions into the function `calculate_cpx_liq_press_temp_matching` (Fig. 6). Step 6 uses matplotlib to plot averaged pressures and temperatures from each Cpx as red diamonds with 1σ error bars (plt.errorbar), and all possible matches as semi-transparent symbols.

7.2 Orthopyroxene-Liquid Thermobarometry

The orthopyroxene-liquid functions in Thermobar are very similar to those for Cpx-Liq. If users wish to calculate pressure or temperature for Opx-Liq pairs (e.g., measured rim and matrix glass compositions), they can use the functions `calculate_opx_liq_press` and `calculate_opx_liq_temp`. Similarly, P and T can be solved iteratively using `calculate_opx_liq_press_temp`, specifying an equationP and equationT.

`calculate_opx_liq_press_temp_matching` assesses all possible Liq and Opx pairs, and calculates P and T for those within user-specified ranges for equilibrium. There is only one commonly used equilbrium test for Opx-Liq pairs, which compares measured values of $K_{D,\ Fe-Mg}^{Opx-Liq}$ to those predicted from the Liq. Putirka [2008] suggest that the range of $K_{D,\ Fe-Mg}$ values in experiments ranges from 0.29±0.06, and can be expressed as a function of the cation fraction of Si in the liquid ($K_{D,\ Fe-Mg}$=0.4805-0.3773 X_{Si}^{liq}). Because this equilibrium test is independent of P and T, Opx-Liq pairs can be filtered without any iteration (simplifying the function relative to that for Cpx-Liq). The Opx-Liq melt matching algorithm follows steps 1-3 described in Section 7.1. Then, $K_{D,\ Fe-Mg}$ values are computed for each Opx-Liq pair, and compared to equilibrium values. By default, the function calculates equilibrium values using the X_{Si}^{liq} expression of Putirka [2008], and considers all matches within $\Delta K_{D,\ Fe-Mg}$ of 0.06. Users can override this default option by specifying a value for `Kd_Match`, and `Kd_Err` in the function. To evaluate Opx-Liq pairs with measured $K_{D,\ Fe-Mg}$=0.29±0.07:

```
pt.calculate_opx_liq_press_temp_matching(
liq_comps=myLiquids, opx_comps=myOpxs,
equationT="T_Put2008_eq28a",
equationP="P_Put2008_eq29b",
Kd_Match=0.29, Kd_Err=0.07)
```

Following this filtering step, the function takes pairs in equilibrium and uses the `calculate_opx_liq_press_temp` function to calculate pressure and temperature for each pair. A dictionary is returned, containing the pressure and temperature for each pair. A second output is also calculated, where all matches for a given orthopyroxene are averaged (e.g., Opx1-Liq1, Opx1-Liq10, Opx1-Liq32). Users also have the option to overwrite the Fe3Fet_Liq value specified in input, as this function uses only Fe^{2+} in the melt to calculate $K_{D,\ Fe-Mg}$.

7.3 Two Pyroxene Thermobarometry

The function `calculate_cpx_opx_temp` allows users to calculate temperatures for matched Cpx-Opx pairs, `calculate_cpx_opx_press` calculates pressures, and `calculate_cpx_opx_press_temp` iterates towards a pressure and temperature. Unlike for Opx-Liq and Cpx-Liq, the function for assessing all possible Cpx-Opx pairs, `calculate_cpx_opx_press_temp_matching`, returns all pairs by default. This is because the partitioning of Fe-Mg between Cpx-Opx is the only available equilibrium test, and this parameter shows a lot of variation between different volcanic systems. We do not intend users to consider all

Step 1 - Import all measured Liquids and Cpxs

```
out=pt.import_excel('Scruggs_Input.xlsx', sheet_name="Liquids")
my_input=out['my_input']
myLiquids1=out['Liqs']

out2=pt.import_excel('Scruggs_Input.xlsx', sheet_name="Cpxs")
my_input2=out2['my_input']
myCpxs1=out2['Cpxs']
```

Extracts df of liquid compositions

Extracts df of cpx compositions

Step 2 - Generate Silicic and Mafic end-members (adding noise)

```
Sil_endmember_noise1=pt.add_noise_sample_1phase(phase_comp=myLiquids1,  duplicates=5, filter_q='SiO2_Liq > 65',
                    phase_err_type="Perc", noise_percent=1, err_dist="normal", append=True)

Maf_endmember_noise1=pt.add_noise_sample_1phase(phase_comp=myLiquids1, duplicates=5, filter_q='SiO2_Liq < 53.8 & MgO_Liq>4',
                    phase_err_type="Perc", noise_percent=1, err_dist="normal", append=True)
```

Creates 5 duplicates per sample

Compositional filter

Appends liqs passing compositional filter to new noisy samples

Add normally distributed noise (1σ=1%)

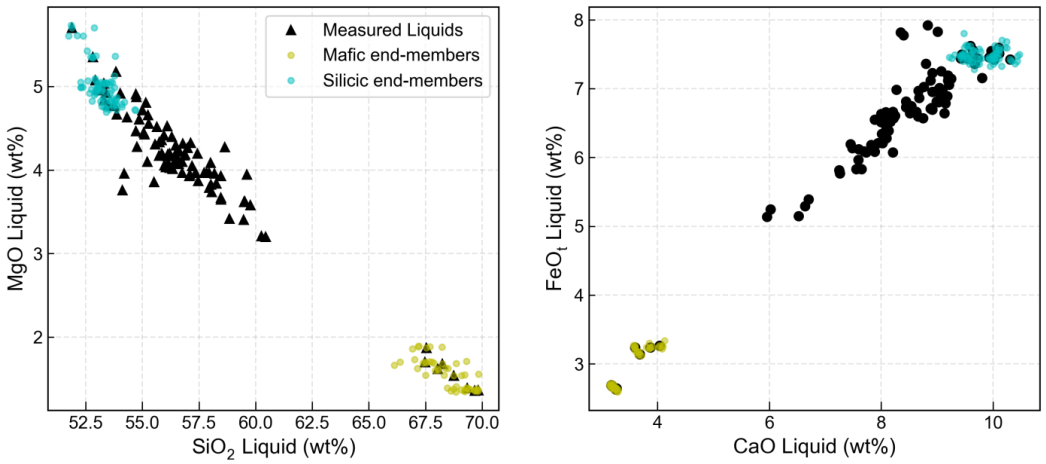

Step 3 - Generate synthetic liquids by mixing end-members

```
Mixed_noise1_selfbig=pt.calculate_bootstrap_mixes(endmember1=Sil_endmember_noise1,
                    endmember2=Maf_endmember_noise1, num_samples = 500, self_mixing = "Partial")
```

50% mixes between end members

50% mixes within each end member

Generates 500 synthetic liquids

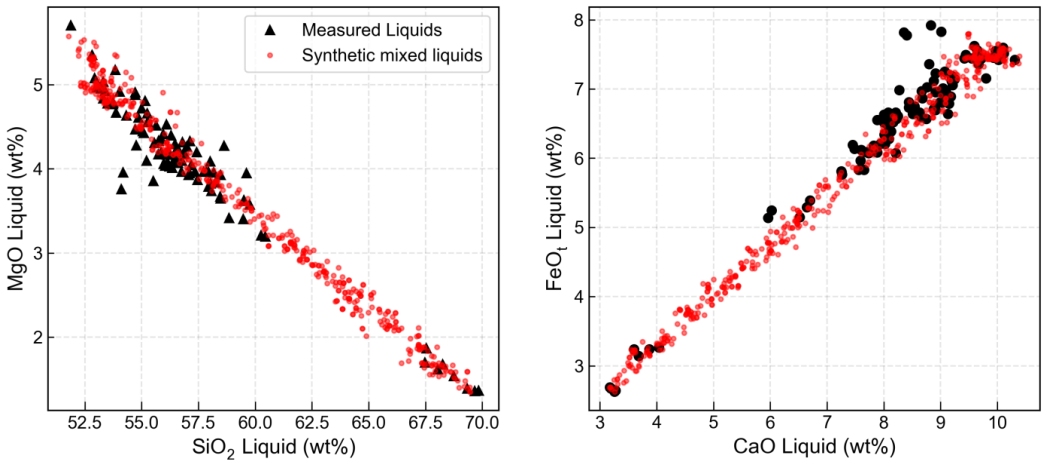

Figure 5: Example of functions allowing users to generate synthetic liquids, adapted from the approach of Scruggs and Putirka [2018]. **Step 1**: The user reads in all measured Cpx compositions into one pandas dataframe (myCpxs1), and all liquids into a second dataframe (MyLiquids1). **Step 2**: Using as many compositional filters as required, the user defines 2 end members. **Step 3**: These end members are then mixed to generate 500 synthetic liquids which incorporate the variation in the natural data.

Step 4 - Combine synthetic liquids and measured liquids ¶

```
Liq_Comp=pd.concat([Mixed_noise1_selfbig.reset_index(drop=True),
        myLiquids1.reset_index(drop=True)], axis=0).reset_index(drop=True).fillna(0)
```

Gets rid of indexing issues, removes Nans

Step 5 - Set water content (following Scruggs and Putirka, 2018)

```
Liq_Comp['H2O_Liq']=Liq_Comp['SiO2_Liq']*0.06995+0.383
```

Overwrites water contents with a value dependent on SiO2

Step 6 - Perform melt matching to calculate pressures and temperatures

```
melt_match_out_syn=pt.calculate_cpx_liq_press_temp_matching(liq_comps=Liq_Comp, cpx_comps=myCpxs1,
                    equationP="P_Neave2017", equationT="T_Put2008_eq33", KdMatch=0.27, KdErr=0.03)
Syn_Avs=melt_match_out_syn['Av_PTs']
Syn_All=melt_match_out_syn['All_PTs']
```

Average P and T per cpx

All Matches

Considers matches with Kd=0.27±0.03

Syn Average dataframe:

	No. of liquids averaged	Sample_ID_Cpx	Mean_T_K_calc	st_dev_T_K_calc	Mean_P_kbar_calc	st_dev_P_kbar_calc	Mean_Delta_Kd_Put2008	Mean_Delta_Kd_Mas2013	Mean_Delta_EnFs	Mean_Delta_CaTs
0	112	12	1306.874096	8.462061	-0.533247	0.411903	0.044293	0.144914	0.042185	0.016345
0	56	16	1281.141557	18.491046	1.390111	0.746137	0.056823	0.149984	0.004690	0.010030
0	5	26	1304.251537	4.271816	0.623434	0.441238	0.024975	0.131124	0.040744	0.028638
0	217	29	1308.642525	11.814991	-0.498931	0.506761	0.016348	0.119370	0.039149	0.010773
0	11	30	1302.787795	7.103075	-0.561921	0.219530	0.047838	0.146350	0.040597	0.021698
...	...	...	...	...	...	...	...	...	...	...

Plotting average for each Cpx, with all matches underlain

```
fig, (ax1) = plt.subplots(1, 1, figsize=(6, 5))
ax1.plot(Syn_All['T_K_calc'],  Syn_All['P_kbar_calc'], 'or',
        ms=2, mfc='red', alpha=0.1, label='All Matches')
ax1.errorbar(Syn_Avs['Mean_T_K_calc'],  Syn_Avs['Mean_P_kbar_calc'],
             xerr=Syn_Avs['st_dev_T_K_calc'],
             yerr=Syn_Avs['st_dev_P_kbar_calc'],
             fmt='d', ecolor='k', elinewidth=0.8,
             mfc='red', ms=8, mec='k', label='Average Matches')
ax1.invert_yaxis()
ax1.set_xlabel('Temp (K)')
ax1.set_ylabel('Pressure (kbar)')
ax1.legend()
fig.savefig('AllMatches_PT.png', dpi=300)
```

Plots light red circles, all cpx-liq matches

Plots error bar for the average PT for each Cpx

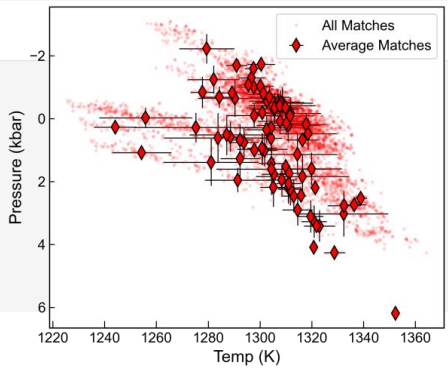

Figure 6: **Step 4**: Once synthetic liquids have been calculated, users may wish to combine them with measured liquid compositions to get the largest number of available comparisons. **Step 5**: Columns in this combined dataframe can be easily overwritten - Here, the liquid H_2O content is calculated from the SiO_2 content of the liquid (following Scruggs and Putirka [2018]). **Step 6**: Once the liquid input is set, the function calculate_cpx_liq_press_temp_matching is called, specifying the choice of liquid and Cpx compositions, as well as the equation for pressure and temperature (Step 6). The function returns a dictionary, which can be subdivided into a pandas dataframe containing all matches, and a dataframe where pressures and temperatures have been averaged for all the liquids in equilibrium with a given Cpx composition. Plotting both outputs gives insight into the amount of scatter associated with each Cpx-Liq pair compared to averaged outputs.

pairs, but instead we strongly encourage them to investigate a suitable equilibrium cut off for their system of interest.

Users can specify a value of `Kd_Match` and `Kd_Err`). Alternatively, specifying `Kd_Match="HighTemp"` will calculate pressures and temperatures for all Cpx-Opx pairs with $K_{D,\ Fe-Mg}^{Cpx-Opx}$=1.09 ± 0.14 (suggested by Putirka [2008] for high temperature systems). Similarly, `Kd_Match="LowTemp"` uses pairs within 0.7 ± 0.2 (for subsolidus systems; Putirka [2008]). As for Cpx- and Opx-Liq, the function returns a dictionary containing pressures and temperatures for all matches, as well as pressures and temperatures averaged for each Cpx, and for each Opx.

7.4 Plagioclase-Liquid and Alkali Feldspar-Liquid Thermobarometery

For Plag-Liq and Kspar-Liq thermobarometry, we use generic functions because the mineral component calculations of Putirka [2008] are the same for all feldspar end-members (`calculate_fspar_liq_temp`, `calculate_fspar_liq_press`, `calculate_fspar_liq_press_temp`). When these functions are used for Plag compositions, the dataframe of oxides should be entered as `plag_comps=" "`, and for Kspars, as `kspar_comps=" "`.

Equilibrium tests are currently only implemented for Plag, comparing the calculated and predicted An, Ab and Or components between Plag and Liq. In particular, Putirka [2008] suggest that the Ab-An exchange coefficient is a good equilibrium test, as it varies little as a function of pressure, temperature or melt H_2O content (~0.27±0.18). In their supporting spreadsheet updated since 2008, they use values of 0.28±0.11 for T>1050°C, and 0.1±0.05 for T<1050°C. In the example Jupyter notebook at Read The Docs, we demonstrate how to filter pairs using this equilibrium criteria.

7.5 Plagioclase Hygrometers

The function `calculate_fspar_liq_hygr` allows the H_2O contents of liquids which crystallized Plag to be estimated. These hygrometers require users to specify the composition of the liquid, as well as the anorthite and albite content of each Plag. Analogous to the other two-phase functions, the composition of Liq and Plag dataframes are specified in the function, along with the pressure and temperature, and choice of equation (here, using the hygrometer of Waters and Lange [2015]):

```
pt.calculate_fspar_liq_hygr(
liq_comps=myLiquids, plag_comps=myPlags,
equationH="H_Waters2015", T=1300, P=5)
```

This returns a pandas dataframe of the calculated H_2O content, along with an indicator of whether the pair passed the recommended equilibrium test of Putirka [2008] based on the temperature input by the user.

	Pass An-Ab Eq Test Put2008?	H2O_calc	Delta_An	Delta_Ab	Delta_Or	Pred_An_EqE
0	Low T: Yes	2.183611	0.056252	0.141146	0.029165	0.360876
1	Low T: Yes	2.671574	0.083157	0.227579	0.028164	0.369968

Alternatively, users can just enter the anorthite and albite content of the Plag without requiring the full Plag composition:

```
pt.calculate_fspar_liq_hygr(
liq_comps=myLiquids, XAn=0.5, XAb=0.4,
equationH="H_Waters2015", T=1300, P=5)
```

As with other optional inputs, XAn and XAb can be a single value, or a panda series with a different value for each row of the calculation.

Plag-Liq hygrometers are very sensitive to temperature. In the Read The Docs example, we show that an increase in temperature from 1100 to 1200 K corresponds to a drop in calculated H_2O contents from 5.85 to 3.64 wt% H_2O. In many cases, temperatures to use with Plag hygrometers are estimated from other mineral pairs (e.g., Fe-Ti oxides, Waters and Lange [2015]). However, there is no guarantee that different mineral phases are recording the same part of the magmatic history, and in many systems, no independent constraint on temperature exists. Given that Plag-Liq equilibra are sensitive to temperature and H_2O content, we incorporate a function into Thermobar which iterates temperature and calculated H_2O content `calculate_fspar_liq_temp_hygr` by specifying a thermometer and hygrometer:

```
Dict_HT=pt.calculate_fspar_liq_temp_hygr(
liq_comps=myLiquids, plag_comps=myPlags,
equationT="T_Put2008_eq23",
equationH="H_Waters2015",
P=5, iterations=30)
```

This function returns a dictionary, comprising two DataFrames:

```
Calc_HT=Dict_HT['T_H_calc']
Evol_HT=Dict_HT['T_H_Evolution']
```

The first DataFrame, indicated by the key `'T_H_calc'`, contains calculated temperatures and H_2O contents, as well as an indication of the change in T and H_2O content between the final iterative step and the penultimate iterative step. If these `Delta` values are small, it indicates sufficient iterations were used. If these numbers

are larger than say 0.01, it indicates that the iteration has not converged. At this point, it is worth inspecting the second output, indicated by the key `'T_H_Evolution'`, which shows the evolution of T and H_2O for each sample against the number of iterations.

7.6 Two Feldspar Thermobarometry

Temperatures from co-existing Kspar-Plag pairs can be calculated using the function `calculate_plag_kspar_temp`. The function `calculate_plag_kspar_temp_matching` considers all possible pairs between a dataframe of Plag compositions, and a dataframe of Kspar compositions. Putirka [2008] suggest that a comparison of activities for An, Ab and Or in Plag and Kspar using the models of Elkins and Grove [1990] can be used as an equilibrium test. However, Putirka [2008] notes that while the values should nominally be zero, further examination of experimental data is required to determine reasonable cut offs. Thermobar returns the difference between these theoretical values and measured values for each pair if `eq_tests=True` (these values are returned automatically for the matching function). We provide a detailed example showing users how they could filter pairs using different values for these equilibrium tests.

8 Converting Pressures to Depths

It can be very useful to convert pressures from thermobarometry into depths below the surface (e.g., to compare to geophysical signals of unrest). This conversion can be done assuming a constant crustal density and the following equations:

$$P = \rho \times g \times H \quad (1)$$

Where P is Pressure in Pa, ρ is the density of the crust in kg/m^3, and H is the height of the crustal column in m (i.e. depth). This equation can be rearranged to calculate height (depth):

$$H = \frac{P}{\rho \times g} \quad (2)$$

Alternatively, a number of parametrizations between pressure and depth that account for varying crustal density are available (e.g. Putirka [2017], Rasmussen et al. [2022], Lerner et al. [2021]). Thus, after calculating pressure using any of the tools in Thermobar, users can easily convert to depth (in km) using a constant crustal density:

```
pt.convert_pressure_to_depth(
P_kbar=Calc_P['P_kbar_calc'],
crust_dens_kgm3=2700)
```

In this instance, `Calc_P` was the dataframe returned from a Cpx-only pressure-temperature iteration

Similarly, one of the available density models can be selected by specifying a model argument (here we choose the average global arc density model derived from seismic data from Rasmussen et al. [2022]):

```
pt.convert_pressure_to_depth(
P_kbar=Calc_P['P_kbar_calc'],
model='rasmussen')
```

Both examples return a panda series of depths in km. This function can be used in a variety of different circumstances to convert depths to pressures, including applications outside of Thermobar (e.g. melt inclusion saturation pressures). Any panda series, numpy array or float/integer can be fet into this function using the argument `P_kbar=...`.

We also provide the option for a different value of the gravitational constant to be specified in the function, so that constant-density calculations and these terrestrial profiles can be applied to other planets (although differences in crustal lithology should be evaluated).

9 Monte-Carlo error propagation

Estimating uncertainty when performing thermobarometry and hygrometery calculations is important, as many calibrations are highly sensitive to the concentration of minor components which are difficult to measure with high precision (e.g., Na_2O in Cpx and Opx). Additionally, sometimes parameters like melt H_2O contents are poorly known, particularly for volcanic systems where melt inclusion analyses are sparse or absent.

The function `add_noise_sample_1phase` can be used to propagate errors in input parameters using Monte-Carlo techniques. This function generates duplicates of rows in a user-inputted dataframe of mineral or liquid compositions with a specified amount of noise added. There are a number of ways to use this function, such as adding uniform or normally distributed noise, inputting percentage or absolute errors (discussed in detail at Read the Docs).

For example, Figure 7 shows a Monte-Carlo simulation propagating analytical errors for measurement of a single Cpx of Gleeson et al. [2020] into a resulting error distribution for pressure and temperature for Cpx-only thermobarometery. Using their analytical conditions, the 1σ error for the Wang et al. [2021] barometer is ±0.39 kbar and ±7 K. For the thermobarometer of Putirka [2008], the 1σ error is ±0.85 kbar and ±10 K. If Na_2O was counted for a shorter time (or using a lower current) during electron microprobe analyses such that the analytical error was twice as large (17%), the 1σ error increases to ±0.62 kbar from Wang et al. [2021],

and ±0.96 kbar from Putirka [2008]. These functions can also be used to assess errors in two phase thermobarometers. Importantly, they allow users to estimate the uncertainty resulting from their specific analytical conditions, and by extension, can be used to decide appropriate EPMA conditions to obtain a certain level of precision. The effect of analytical errors on Cpx-based barometry sing these Monte Carlo functions is discussed in detail in Wieser et al. (in review).

10 Single garnet xenocryst thermobarometry

Thermobarometric calculations of peridotitic garnet xenocrysts are widely used to determine the thermal structure of the underlying lithospheric mantle. The composition of the peridotitic garnet can be used as a diamond indicator (Grütter et al. [2004]) and to depict the style of mantle metasomatism (Griffin et al. [2002]). Garnet thermometers utilize the strong temperature dependence on Ni-partitioning between garnet and olivine (Ryan et al. [1996], Canil [1999], Sudholz et al. [2021]). Geobarometers, on the other hand, are based on Cr-solubility in coexisting garnet and hypothetical peridotitic orthopyroxene (Ryan et al. [1996]). Thermometers and geobarometers in Thermobar can be calculated with the functions `calculate_gt_temp` and `calculate_gt_press`, respectively, after a user loads in garnet compositions from a spreadsheet with `_Gt` suffixes.

Constructing a geotherm with garnet thermobarometry is different to conventional curve-fitting methods. First, one must construct generalised continental geotherms (Pollack and Chapman [1977], Hasterok and Chapman [2011]) and select a well-fitting one dependent on the locus defined by the maximum pressures. This is because not all garnets would potentially satisfy the Cr-saturation (in equilibrium with Cr-spinel) condition and are likely to underestimate the pressures. For this reason, the best determination can be made with depleted garnets with more numerous Cr-spinel temperatures. To determine the depths of these garnets, they have to be projected vertically down to the constructed continental geotherm. The constructed geotherms can be chosen to be kinked at the temperature at the base of the depleted lithosphere, which can be determined by a sudden population decrease of depleted garnets (Y-in-garnet < 10 ppm). The temperatures after this point are not well-constrained and can be assumed to follow a kinked geotherm parallel to the diamond-graphite transition since they seem to follow that trend Griffin et al. [2003]. This possibly indicates a local and temporal disturbance of the geotherm inflicted by a heat source (Ryan et al. [1996], Griffin et al. [2003]). These calculations can

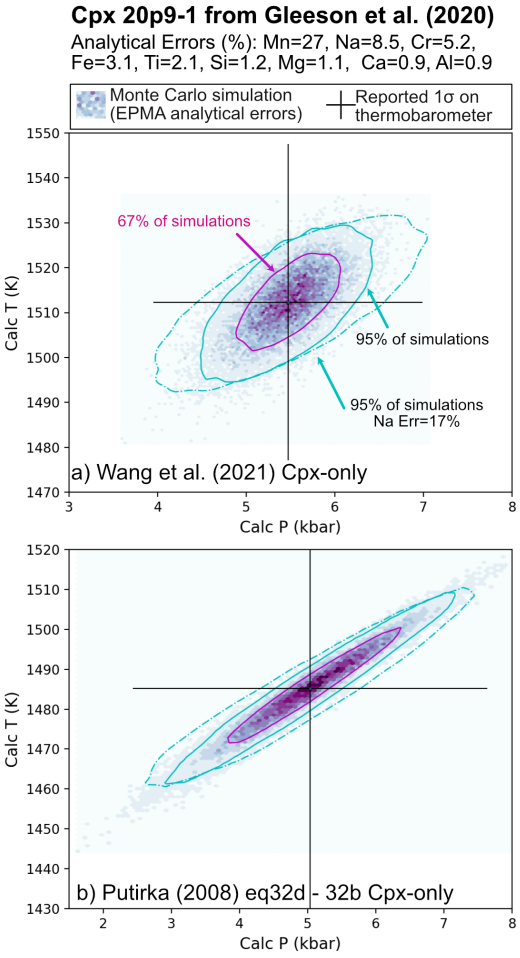

Figure 7: Propagated analytical errors from EPMA analyses into resulting distributions of pressures and temperatures. 1σ errors obtained from EPMA software during the analysis of a Cpx from Gleeson et al. [2020] with 0.38 wt% Na_2O was used to make 20,000 synthetic Cpx compositions. Pressures and temperature were then calculated using the Cpx-only thermobarometers of Wang et al. [2021] (eq1 and eq2) and Putirka [2008] (eq32d-32b). These results are colored using the hexbin function, and contours around 67% and 95% of the data are overlain using Pyrolite (Williams et al. [2020]). We also show the 95% contour calculated for an analytical error on Na twice that reported by Gleeson et al. [2020].

be made via the function `plot_garnet_geotherm`.

10.1 Garnet Chemical Tomography

Garnet data and constructed garnet-based paleogeotherms can be utilised to depict the compositional structure of the underlying lithospheric mantle with several methods (Griffin et al. [2002]). These classifications can be carried out and plotted with the function `plot_garnet_composition_section` function in the `garnet_plot module`. To use this functionality, one needs to have the additional trace element data in addition to the major element composition.

10.2 Garnet Chemical Tomography

Garnet data and constructed garnet-based paleogeotherms can be utilised to depict the compositional structure of the underlying lithospheric mantle with several methods (Griffin et al. [2002], Grütter et al. [2004]). These classifications can be carried out and plotted with the function `plot_garnet_composition_section`. To use this functionality, one needs to have the additional trace element data in addition to the major composition (X, Y, Z).

10.3 Generalized Continental Geotherms

Generalised continental geotherms are useful in determining the temperature structure from thermobarometric data. Thermobar makes use of the generalised continental geotherms of Hasterok and Chapman [2011], which can be calculated with the function `calculate_hasterok2011_geotherm`. This can be combined with the adiabatic temperature profile from Katsura [2022] to determine the lithosphere-asthenosphere boundary. The function `invert_generalised_mantle_geotherm` can be used to invert a generalised continental geotherm's surface heat flow value for the input thermobarometric data.

11 Integration with other open-source Python tools

In the last few years, there has been an increase in the number of petrological tools available in python (e.g., Pyrolite for geochemical plotting: Williams et al. [2020], MiMIC for melt inclusion modification: Rasmussen et al. [2020], VESIcal for volatile solubility: Iacovino et al. [2021]). Having thermobarometery tools available in python through Thermobar will allow increased integration between various codes. For example, one of the most common uses of volatile solubility models is to calculate the pressure at which a melt inclusion was trapped based on reconstructing its H_2O, CO_2, and major element contents at the time of melt inclusion entrapment. To convert these chemical parameters into a pressure, the temperature of the melt inclusion at the time of entrapment must also be estimated. On Read The Docs and YouTube, we show how the functions `convert_to_VESIcal` and `convert_from_VESIcal` can be used to convert oxide data back and forth from the formats used in Thermobar and VESIcal so the tools can be used together.

12 Future Work

The open-source nature of Thermobar, with code available on GitHub, means that users can adapt functions, add their own, or incorporate new thermobarometery or hygrometry equations as they are published. Authors publishing new thermobarometry equations can contact the author team of Thermobar, and an effort will be made to continue to update the available equations. To reflect the probable evolving nature of this tool, when citing Thermobar, users should specify which version they used, as well as citing the original equations used for calculations. For example "Cpx-Liq pressures and temperatures were calculated using equation 30 and 31 of Putirka (2008), implemented through the python3 tool Thermobar (version 1.0.1, Wieser et al. 2021)". The version can be found after importing Thermobar by running the command:

```
pt.__version__
```

Ideally, users should provide the Jupyter notebook used for calculations for maximum reproducibility, and to outline the various options used (particularly for more complicated operation such as melt matching, error propagation).

13 Conclusions

Thermobar is a new tool that provides access to more than 100 popular thermometers, barometers and hygrometers through easy-to-implement and customizable functions within the open-source programming language, Python3. Users can easily change the equation, pressure, temperature, proportion of Fe^{3+} and water content of calculations, iterate towards a solution when neither pressure nor temperature is known, compute equilibrium tests, and assess all possible matches of equilibrium pairs (Cpx-Liq, Opx-Cpx, Opx-Liq, Fspar-Liq) in a single line of code. The functionality of this tool will allow more robust interpretation of the systematic and random errors associated with thermobarometry and hygrometry in igneous systems. For example, the design of the functions means that users can

easily switch between equations to investigate systematic differences between published parametrizations. The Monte-Carlo error propagation functions allow users to assess the amount of random error introduced by their specific analytical protocol, which complements published uncertainty estimates for each equation. The fact that users can publish their workflows in a single Jupyter Notebook (rather than a myriad of different tools) will help to make thermobarometry calculations more reproducible.

Acknowledgements

We are very grateful to Keith Putirka for answering a lot of questions about the implementation of different barometers in his Excel spreadsheets, as well as very helpful discussions regarding $K_{D,\ Fe\text{–}Mg}$. We thank Euan Mutch for sharing a spreadsheet for his amphibole barometer, and David Neave for helpful discussions regarding his melt-matching tool. PW thanks Kayla Iacovino and Simon Matthews for introducing her to the wonderful world of developing open-source python tools. This contribution was supported by funding from National Science Foundation grants 1948862 and 1949173 to AJRK and CBT, and start up funds to PW from UC Berkeley.

Liquid-only thermometry

Function: "calculate_liq_only_temp"

Reference	Name in ThermoBar	P-dependent?	H_2O-dependent?
Olivine-Sat Liquids			
Putirka (2008)	T_Put2008_eq13	✗	✗
	T_Put2008_eq14	✗	✓
	T_Put2008_eq15	✓	✓
Helz & Thornber, (1987)	T_Helz1987_MgO	✗	✗
Montierth (1995)	T_Montierth1995_MgO	✗	✗
Sugawara (2000)	T_Sug2000_eq1	✗	✗
	T_Sug2000_eq3_ol	✓	✗
	T_Sug2000_eq6a	✓	✗
	T_Sug2000_eq6a_H7a	✓	✓
Beattie (1993)	T_Beatt93_ BeattDMg	✓	✗
	T_Beatt93_BeattDMg_HerzCorr	✓	✗
Putirka (2008)	T_Put2008_eq19_BeattDMg	✓	✗
	T_Put2008_eq21_BeattDMg	✓	✓
	T_Put2008_eq22_BeattDMg	✓	✓
Cpx-Sat Liquids			
Putirka (2008)	T_Put2008_eq34_cpx_sat	✓	✓
Putirka (1999)	T_Put1999_cpx_sat	✓	✗
Sugawara (2000)	T_Sug2000_eq3_cpx	✓	✗
	T_Sug2000_eq3_pig	✓	✗
	T_Sug2000_eq6b	✓	✗
	T_Sug2000_eq6b_H7b	✓	✓
Opx-Sat Liquids			
Putirka (2008)	T_Put2008_eq28b_opx_sat	✓	✓
Sugawara (2000)	T_Sug2000_eq3_opx	✓	✗
Beattie (1993)	T_Beatt1993_opx	✓	✗
Amp-Sat Liquids			
Putirka (2008)	T_Put2016_eq3_amp_sat	✗	✓*
Molina (2015)	T_Molina2015_amp_sat	✗	✗
Fspar-Sat Liquids			
Putirka (2005)	T_Put2005_eqD_plag_sat	✓	✓
Putirka (2008)	T_Put2008_eq26_plag_sat	✓	✓
	T_Put2008_eq24c_kspar_sat	✓	✓
Ol-Cpx-Plag Sat Liquids			
Putirka (2008)	T_Put2008_eq16	✓	✗
Helz & Thornber (1987)	T_Helz1987_CaO	✗	✗

Figure 8: Summary of equations for liquid-only thermometry. *Note, Putirka [2016] equation 3 doesn't contain a H_2O term, but is H_2O-sensitive because liquid cation fractions are calculated on a hydrous basis. Equations from: Putirka [2008], Sugawara [2000], Montierth et al. [1995], Helz and Thornber [1987], Beattie [1993], Herzberg and O'hara [2002], Putirka [1999], Molina et al. [2015], Putirka [2016]

Olivine Thermometers and Hygrometers

Reference	Name in ThermoBar	T-dependent?	P-dependent?	H_2O-dependent?
Olivine-Liquid thermometry. *Function "calculate_ol_liq_temp"*				
Putirka (2008)	T_Put2008_eq19		✓	✗
	T_Put2008_eq21		✓	✓
	T_Put2008_eq22		✓	✓
Beattie (1993)	T_Beatt93_ol		✓	✗
	T_Beatt93_ol_HerzCorr		✓	✗
Sisson and Grove (1992)	T_Sisson1992		✓	✗
Pu et al. (2017)	T_Pu2017		✗	✗
Pu et al. (2021)	T_Pu2021		✓	✗
Olivine-Liquid hygrometers. *Function "calculate_ol_liq_hygr"*				
Gavrilenko et al. (2016)	H_Gavr2016	✗	✗	
Olivine-Spinel thermometry. *Function "calculate_ol_sp_temp"*				
Coogan et al. (2014)	T_Coogan2014		✗	✗
Wan et al. (2008)	T_Wan2008		✗	✗

Feldspar Thermometers, Barometers and Hygrometers

Phase	Reference	Name in ThermoBar	T-dependent?	P-dependent?	H_2O-dependent?
Feldspar-Liquid thermometry. *Function "calculate_fspar_liq_temp"*					
Plag-Liq	Putirka (2008)	T_Put2008_eq23		✓	✓
		T_Put2008_eq24a		✓	✓
Kspar-Liq	Putirka (2008)	T_Put2008_eq24b		✓	✗
Feldspar-Liquid barometry. *Function "calculate_fspar_liq_press"*					
Plag-Liq	Putirka (2008)	P_Put2008_eq25	✓		✗
Feldspar-Liquid hygrometry. *Function "calculate_fspar_liq_hygr"*					
Plag-Liq	Putirka (2008)	H_Put2008_eq25b	✓	✓	
	Putirka (2005)	H_Put2005_eqH	✓	✗	
	Waters & Lange (2015)	H_Waters2015	✓	✓	
	Masotta et al. (2019)	H_Masotta2019	✓	✗	
Two Feldspar thermometry. Function "calculate_plag_kspar_temp"					
Plag-Kspar	Putirka (2008)	T_Put2008_eq27a		✓	✗
		T_Put2008_eq27b		✓	✗
		T_Put_Global_2Fspar		✓	✗

Figure 9: Summary of equations for olivine-liquid and olivine-spinel thermometry, olivine-liquid hygrometry, feldspar thermobarometry and hygrometry. From: Putirka [2008], Beattie [1993], Herzberg and O'hara [2002], Sisson and Grove [1993], Pu et al. [2021], Pu et al. [2017], Wan et al. [2008], Coogan et al. [2014], Gavrilenko et al. [2016], Putirka [2005], Waters and Lange [2015].

Clinopyroxene-Liquid Thermobarometers

Reference	Name in ThermoBar	T-dependent?	P-dependent?	H_2O-dependent?
Clinopyroxene-Liquid Barometry. *Function "calculate_cpx_liq_press"*				
Putirka (1996)	P_Put1996_eqP1	✓		✗
	P_Put1996_eqP2	✓		✗
Putirka (2003)	P_Put2003	✓		✗
Putirka (2008)	P_Put2008_eq30	✓		✓
	P_Put2008_eq31	✓		✓
	P_Put2008_eq32c	✓		✓
Masotta et al. (2013) *recalibration of Putirka eqs. for alkali systems*	P_Mas2013_eqPalk1	✓		✗
	P_Mas2013_eqPalk2	✓		✗
	P_Mas2013_eqalk32c	✓		✓
Masotta et al. (2013)	P_Mas2013_Palk2012	✗		✓
Neave & Putirka (2017)	P_Neave2017	✓		✗
Petrelli et al. (2021)	P_ Petrelli2021_Cpx_Liq	✗		✓
Jorgenson et al. (2021)	PlaceHolder			
Clinopyroxene-Liquid Thermometry. *Function "calculate_cpx_liq_temp"*				
Putirka (1996)	T_Put1996_eqT1		✗	✗
	T_Put1996_eqT2		✓	✗
Putirka (1999)	T_Put1999		✓	✗
Putirka (2003)	T_Put2003		✓	✗
Putirka (2008)	T_Put2008_eq33		✓	✓
Masotta et al. (2013) *Recalibration of Putirka eqs. for alkali systems*	T_Mas2013_eqTalk1		✗	✗
	T_Mas2013_eqTalk2		✓	✗
	T_Mas2013_eqalk33		✓	✓
Masotta et al. (2013)	T_Mas2013_Talk2012		✗	✓
Brugman & Till (2019)	T_Brug2019		✗	✗
Petrelli et al. (2020)	T_ Petrelli2020_Cpx_Liq		✗	✓
Jorgenson et al. (2022)	T_Jorgenson2022_Cpx_Liq		✗	✗
Other Functions				
calculate_cpx_liq_press_temp(): Iteratively solves P and T for cpx-liq pairs. **calculate_cpx_liq_press_temp_matching():** Calculates P and T for all possible cpx-liquid pairs **calculate_cpx_rhodes_diagram_lines():** Calculates equilibrium lines for a range of melt Mg#s.				

Clinopyroxene-only Thermobarometers

Reference	Name in ThermoBar	T-dependent?	P-dependent?	H_2O-dependent?
Clinopyroxene-only Barometry. *Function "calculate_cpx_only_press"*				
Putirka (2008)	P_Put2008_eq32a	✓		✗
	P_Put2008_eq32b	✓		✓
Petrelli et al. (2020)*	P_Petrelli2020_Cpx_only	✗		✗
	P_Petrelli2020_Cpx_only_withH2O*	✗		✓
Wang et al. (2021)	P_Wang2021_eq1	✗		✗
	P_Wang2021_eq3	✗		✗
Jorgenson et al. (2022)	P_Jorgenson2022_Cpx_Only	✗		✗

Continued over page...

1713

Reference	Name in ThermoBar	T-dependent?	P-dependent?	H_2O-dependent?
Clinopyroxene-only Thermometry. *Function "calculate_cpx_only_temp"*				
Putirka (2008)	T_Put2008_eq32d		✓	✗
	T_Put2008_eq32d_subsol		✓	✗
Petrelli et al. (2020)	T_Petrelli2020_Cpx_only*		✗	✗
	T_Petrelli2020_Cpx_only_withH2O*		✗	✓
Wang et al. (2021)	T_Wang2021_eq2		✗	✓
	T_Wang2021_eq4		✗	✓
Jorgenson et al. (2022)	T_Jorgenson2022_Cpx_only		✗	✗
Other Functions				
calculate_cpx_only_press_temp(): Iteratively solves P and T using just Cpx compositions				

Orthopyroxene Thermobarometers

Reference	Name in ThermoBar	T-dependent?	P-dependent?	H_2O-dependent?
Orthopyroxene-Liquid Barometry. *Function "calculate_opx_liq_press"*				
Putirka (2008)	P_Put2008_eq29a	✓		✓
	P_Put2008_eq29b	✓		✓
Putirka Supplement New "Global" calibrations	P_Put_Global_Opx	✗		✗
	P_Put_Felsic_Opx	✗		✗
Orthopyroxene-Liquid Thermometry. *Function "calculate_opx_liq_temp"*				
Putirka (2008)	T_Put2008_eq28a		✓	✓
	T_Put2008_eq28b_opx_sat		✓	✓
Orthopyroxene-only Barometry. Function "calculate_opx_only_press"				
Putirka (2008)	P_Put2008_eq29c	✓		✗
Other Functions				
calculate_opx_liq_press_temp(): Iteratively solves P and T for opx-liq pairs. **calculate_opx_liq_press_temp_matching():** Calculates P and T for all possible opx-liquid pairs.**calculate_opx_rhodes_diagram_lines():** Calculates equilibrium lines for a range of melt Mg#s				

Two pyroxene Thermobarometers

Reference	Name in ThermoBar	T-dependent?	P-dependent?	H_2O-dependent?
Orthopyroxene-Clinopyroxene Barometry. *Function "calculate_cpx_opx_press"*				
Putirka (2008)	P_Put2008_eq38	✗		✗
	P_Put2008_eq39	✓		✗
Orthopyroxene-Clinopyroxene Thermometry. *Function "calculate_cpx_opx_press"*				
Putirka (2008)	T_Put2008_eq36		✓	✗
	T_Put2008_eq37		✓	✗
Brey and Kohler (1990)	T_Brey1990		✓	✗
Wells (1977)	T_Wells1977		✗	✗
Wood and Banno (1973)	T_Wood1973		✗	✗
Other Functions				
calculate_cpx_opx_press_temp(): Iteratively solves P and T for opx-cpx pairs.				

Figure 10: Summary of equations for Cpx and Opx thermobarometry. From: Putirka et al. [1996], Putirka et al. [2003], Putirka [2008], Masotta et al. [2013], Neave and Putirka [2017], Brugman and Till [2019], Petrelli [2021], Wang et al. [2021], Jorgenson et al. [2021], Brey and Köhler [1990], Wells [1977], Wood and Banno [1973]. The "Global" and "Felsic" orthopyroxene barometers are from the spreadsheets available at `http://www.fresnostate.edu/csm/ees/faculty-staff/putirka.html`. These equations are particularly-suited to low pressure, low-Al orthopyroxenes where other equations return a numerical error

Amphibole Thermobarometers

Reference	Name in Thermobar	T-dependent?	P-dependent?	H_2O-dependent?
Amphibole-Liquid Barometry. *Function "calculate_amp_liq_press"*				
Putirka (2016)	P_Put2016_eq7a	✗		✓
	P_Put2016_eq7b	✗		✓*
	P_Put2016_eq7c	✗		✓*
Amphibole-Liquid Thermometry. *Function "calculate_amp_liq_temp"*				
Putirka (2016)	T_Put2016_eq4b		✗	✓
	T_Put2016_eq4a_amp_sat		✗	✓*
	T_Put2016_eq9		✗	✓*
Amphibole-only Barometry. *Function "calculate_amp_only_press"*				
Ridolfi and Renzulli (2012)	P_Ridolfi2012_1a	✗		✗
	P_Ridolfi2012_1b	✗		✗
	P_Ridolfi2012_1c	✗		✗
	P_Ridolfi2012_1d	✗		✗
	P_Ridolfi2012_1e	✗		✗
Ridolfi et al. (2010)	P_Ridolfi2010	✗		✗
Hammarstrom & Zen (1986)	P_Hammerstrom1986_eq1	✗		✗
	P_Hammerstrom1986_eq2	✗		✗
	P_Hammerstrom1986_eq3	✗		✗
Hollister et al. (1987)	P_Hollister1987	✗		✗
Johnson & Rutherford (1989)	P_Johnson1989	✗		✗
Blundy et al. (1990)	P_Blundy1990	✗		✗
Schmidt (1992)	P_Schmidt1992	✗		✗
Anderson & Smith, 1995	P_Anderson1995	✓		✗
Krawczynski et al.(2012)	P_Kraw2012	✗		✗
Amphibole-only Thermometry. *Function "calculate_amp_only_temp"*				
Putirka (2016)	T_Put2016_eq5		✗	✗
	T_Put2016_eq6		✗	✗
	T_Put2016_SiHbl		✗	✗
	T_Put2016_eq8		✓	✗
Ridolfi and Renzuli, 2012	T_Ridolfi2012		✓	✗

✓* H_2O-dependence because of parameterization in terms of hydrous fractions, not a specific H_2O-term

Other Functions

***calculate_amp_liq_press_temp*:** Iteratively solves P and T for liquid-amphibole pairs

calculate_amp_only_press_temp: Iteratively solves P and T using just amphibole compositions.

Figure 11: Summary of equations for amphibole thermobarometry. From: Ridolfi [2021], Putirka [2016], Mutch et al. [2016], Krawczynski et al. [2012], Ridolfi and Renzulli [2012], Hollister et al. [1987], Ridolfi et al. [2010], Hammarstrom and Zen [1986], Johnson [1988], Blundy and Holland [1990], Schmidt [1992], Anderson and Smith [1995].

Amphibole Chemometers

Reference	Melt parameter	Output name	T-dependent?
Amphibole-only Chemometry. *Function "calculate_amp_only_melt_comps"* Returns all equations by default			
Ridolfi (2021)	ΔNNO	deltaNNO_Ridolfi21	✗
	H_2O	H2O_Ridolfi21	✗
Zhang et al. (2017)	SiO_2 (Eq 1)	SiO2_Eq1_Zhang17	✗
	SiO_2 (Eq 2)	SiO2_Eq2_Zhang17	✗
	SiO_2 (Eq 3)	SiO2_Eq3_Zhang17	✓
	SiO_2 (Eq 4)	SiO2_Eq4_Zhang17	✗
	TiO_2 (Eq 5)	TiO2_Eq5_Zhang17	✓
	TiO_2 (Eq 6)	TiO2_Eq6_Zhang17	✗
	FeO (Eq 7)	FeO_Eq7_Zhang17	✗
	FeO (Eq 8)	FeO_Eq8_Zhang17	✗
	MgO (Eq 9)	MgO_Eq9_Zhang17	✗
	CaO (Eq 10)	CaO_Eq10_Zhang17	✗
	CaO (Eq 11)	CaO_Eq11_Zhang17	✗
	K_2O (Eq 12)	K2O_Eq12_Zhang17	✗
	K_2O (Eq 13)	K2O_Eq13_Zhang17	✗
	Al_2O_3 (Eq 14)	Al2O3_Eq14_Zhang17	✗
Putirka (2016)	SiO2 (Eq 10)	SiO2_Eq10_Put2016	✓

Figure 12: Summary of equations for amphibole chemometers. From: Putirka [2016], Zhang et al. [2017], and Ridolfi [2021].

Author contributions

PW and MP conceived the project, with help from AK and CT. PW wrote the manuscript, documentation, examples and the majority of the python code, as well as performing the benchmarking of this code to existing tools. MP and JL helped with aspects of code writing (e.g., MP-bootstrapped liquids and JL-amphibole site occupancy, boundaries for Fspar classification diagrams), as well as code testing and debugging. SO wrote the functions involving garnet and geotherms, and PW merged it into Thermobar. EW helped optimize computational speed for various iterative calculations, as well as providing guidance for writing documentation in sphinx, creating a binder file, and making the code available through pip. All authors provided feedback on the manuscript.

Data availability

All files are available on GitHub (https://github.com/PennyWieser/Thermobar), with documentation and examples at Read The Docs (https://readthedocs.org/projects/thermobar/ - latest version of code found by clicking on "latest"). The code can be run through binder on Read The Docs. YouTube videos explaining various aspects of the tool are available on the Thermobar channel (https://www.youtube.com/channel/UC7ddceuNnikCdQa_fRHmdXw).

References

Anderson, J. L. and Smith, D. R. (1995). The effects of temperature and fo2 on the al-in-hornblende barometer. *American Mineralogist*, 80(5-6):549–559.

Andrews, B. J., Befus, K. S., Blatter, D. L., Coombs, M. L., deGraffenried, R., Hammer, J. E., Gardner, J. E., Larsen, J. F., Shea, T., and Wright, H. M. N. (2019). Rapid experimental determination of magmatic phase equilibria: coordinating a volcanic crisis response protocol. In *AGU Fall Meeting Abstracts*, volume 2019, pages V33A–03.

Bachmann, O. and Dungan, M. A. (2002). Temperature-induced al-zoning in hornblendes of the fish canyon magma, colorado. *American Mineralogist*, 87(8-9):1062–1076.

Balta, J. B., Sanborn, M., McSween Jr, H. Y., and Wadhwa, M. (2013). Magmatic history and parental melt composition of olivine-phyric shergottite lar 06319: Importance of magmatic degassing and olivine antecrysts in martian magmatism. *Meteoritics & Planetary Science*, 48(8):1359–1382.

Beattie, P. (1993). Olivine-melt and orthopyroxene-melt equilibria. *Contributions to Mineralogy and Petrology*, 115(1):103–111.

Blundy, J. D. and Holland, T. J. (1990). Calcic amphibole equilibria and a new amphibole-plagioclase geothermometer. *Contributions to mineralogy and petrology*, 104(2):208–224.

Brey, G. P. and Köhler, T. (1990). Geothermobarometry in four-phase lherzolites ii. new thermobarometers, and practical assessment of existing thermobarometers. *Journal of Petrology*, 31(6):1353–1378.

Brugman, K. K. and Till, C. B. (2019). A low-aluminum clinopyroxene-liquid geothermometer for high-silica magmatic systems. *American Mineralogist: Journal of Earth and Planetary Materials*, 104(7):996–1004.

Canil, D. (1999). The ni-in-garnet geothermometer: calibration at natural abundances. *Contributions to Mineralogy and Petrology*, 136(3):240–246.

Caricchi, L., Petrelli, M., Bali, E., Sheldrake, T., Pioli, L., and Simpson, G. (2020). A data driven approach to investigate the chemical variability of clinopyroxenes from the 2014–2015 holuhraun–bárdarbunga eruption (iceland). *Frontiers in Earth Science*, 8:18.

Coogan, L., Saunders, A., and Wilson, R. (2014). Aluminum-in-olivine thermometry of primitive basalts: Evidence of an anomalously hot mantle source for large igneous provinces. *Chemical Geology*, 368:1–10.

Cooper, K. M. (2019). Time scales and temperatures of crystal storage in magma reservoirs: Implications for magma reservoir dynamics. *Philosophical Transactions of the Royal Society A*, 377(2139):20180009.

Culha, C., Suckale, J., Keller, T., and Qin, Z. (2020). Crystal fractionation by crystal-driven convection. *Geophysical Research Letters*, 47(4):e2019GL086784.

Deer, W. A., Howie, R. A., and Zussman, J. (1992). An introduction to the rock-forming minerals, 3rd edition. Geological Society of London.

Ducea, M. N., Saleeby, J. B., and Bergantz, G. (2015). The architecture, chemistry, and evolution of continental magmatic arcs. *Annual Review of Earth and Planetary Sciences*, 43:299–331.

Elkins, L. T. and Grove, T. L. (1990). Ternary feldspar experiments and thermodynamic models. *American Mineralogist*, 75(5-6):544–559.

Evans, B. W., Hildreth, W., Bachmann, O., and Scaillet, B. (2016). In defense of magnetite-ilmenite thermometry in the bishop tuff and its implication for gradients in silicic magma reservoirs. *American Mineralogist*, 101(2):469–482.

Gaetani, G. A., O'Leary, J. A., Shimizu, N., Bucholz, C. E., and Newville, M. (2012). Rapid reequilibration of h_2o and oxygen fugacity in olivine-hosted melt inclusions. *Geology*, 40(10):915–918.

Gavrilenko, M., Herzberg, C., Vidito, C., Carr, M. J., Tenner, T., and Ozerov, A. (2016). A calcium-in-olivine geohygrometer and its application to subduction zone magmatism. *Journal of Petrology*, 57(9):1811–1832.

Ghiorso, M. S. and Prissel, K. B. (2020). Enki cloud app: Implementation of the fe-ti oxide geothermooxybarometer of ghiorso and evans, 2008. *10.5281/zenodo.3866660*, page 1033.

Giordano, D., Russell, J. K., and Dingwell, D. B. (2008). Viscosity of magmatic liquids: a model. *Earth and Planetary Science Letters*, 271(1-4):123–134.

Gleeson, M. L., Gibson, S. A., and Stock, M. J. (2020). Upper mantle mush zones beneath low melt flux ocean island volcanoes: insights from isla floreana, galápagos. *Journal of Petrology*, 61(11-12):egaa094.

Griffin, W., Fisher, N., Friedman, J., O'Reilly, S. Y., and Ryan, C. (2002). Cr-pyrope garnets in the lithospheric mantle 2. compositional populations and their distribution in time and space. *Geochemistry, Geophysics, Geosystems*, 3(12):1–35.

Griffin, W., O'Reilly, S. Y., Natapov, L., and Ryan, C. (2003). The evolution of lithospheric mantle beneath the kalahari craton and its margins. *Lithos*, 71(2-4):215–241.

Grütter, H. S., Gurney, J. J., Menzies, A. H., and Winter, F. (2004). An updated classification scheme for mantle-derived garnet, for use by diamond explorers. *Lithos*, 77(1-4):841–857.

Gualda, G. A. and Ghiorso, M. S. (2014). Phase-equilibrium geobarometers for silicic rocks based on rhyolite-melts. part 1: Principles, procedures, and evaluation of the method. *Contributions to Mineralogy and Petrology*, 168(1):1033.

Hammarstrom, J. M. and Zen, E.-a. (1986). Aluminum in hornblende: an empirical igneous geobarometer. *American mineralogist*, 71(11-12):1297–1313.

Harmon, L. J., Cowlyn, J., Gualda, G. A., and Ghiorso, M. S. (2018). Phase-equilibrium geobarometers for silicic rocks based on rhyolite-melts. part 4: plagioclase, orthopyroxene, clinopyroxene, glass geobarometer, and application to mt. ruapehu, new zealand. *Contributions to Mineralogy and Petrology*, 173(1):7.

Harris, C. R., Millman, K. J., van der Walt, S. J., Gommers, R., Virtanen, P., Cournapeau, D., Wieser, E., Taylor, J., Berg, S., Smith, N. J., et al. (2020). Array programming with numpy. *Nature*, 585(7825):357–362.

Hasterok, D. and Chapman, D. S. (2011). Heat production and geotherms for the continental lithosphere. *Earth and Planetary Science Letters*, 307(1-2):59–70.

Helz, R. T. and Thornber, C. R. (1987). Geothermometry of kilauea iki lava lake, hawaii. *Bulletin of volcanology*, 49(5):651–668.

Herzberg, C. and O'hara, M. (2002). Plume-associated ultramafic magmas of phanerozoic age. *Journal of Petrology*, 43(10):1857–1883.

Hirschmann, M., Ghiorso, M., Davis, F., Gordon, S., Mukherjee, S., Grove, T., Krawczynski, M., Medard, E., and Till, C. (2008). Library of experimental phase relations (lepr): A database and web portal for experimental magmatic phase equilibria data. *Geochemistry, Geophysics, Geosystems*, 9(3).

Hollister, L. S., Grissom, G., Peters, E., Stowell, H., and Sisson, V. (1987). Confirmation of the empirical correlation of al in hornblende with pressure of solidification of calc-alkaline plutons. *American Mineralogist*, 72(3-4):231–239.

Hunter, J. D. (2007). Matplotlib: A 2d graphics environment. *Computing in Science & Engineering*, 9(3):90–95.

Iacovino, K., Matthews, S., Wieser, P. E., Moore, G., and Bégué, F. (2021). Vesical part i: An open-source thermodynamic model engine for mixed volatile (h2o-co2) solubility in silicate melts. *Earth and Space Science*, 8(11):e2020EA001584.

Johnson, M. (1988). Experimental calibration of an aluminum-in-hornblende geobarometer applicable to calc-alkaline rocks. *Eos*, 69:1511.

Jorgenson, C., Higgins, O., Petrelli, M., Bégué, F., and Caricchi, L. (2021). A machine learning based approach to clinopyroxene thermobarometry: model optimisation and distribution for use in earth sciences. *Journal of Geophysical Research: Solid Earth*, page e2021JB022904.

Katsura, T. (2022). A revised adiabatic temperature profile for the mantle. *Journal of Geophysical Research: Solid Earth*, 127(2):e2021JB023562.

Krawczynski, M. J., Grove, T. L., and Behrens, H. (2012). Amphibole stability in primitive arc magmas: effects of temperature, h 2 o content, and oxygen fugacity. *Contributions to Mineralogy and Petrology*, 164(2):317–339.

Leake, B. E., Woolley, A. R., Arps, C. E., Birch, W. D., Gilbert, M. C., Grice, J. D., Hawthorne, F. C., Kato, A., Kisch, H. J., Krivovichev, V. G., et al. (1997). Nomenclature of amphiboles; report of the subcommittee on amphiboles of the international mineralogical association commission on new minerals and mineral names. *Mineralogical magazine*, 61(405):295–310.

Lee, C.-T. A. and Anderson, D. L. (2015). Continental crust formation at arcs, the arclogite "delamination" cycle, and one origin for fertile melting anomalies in the mantle. *Science Bulletin*, 60(13):1141–1156.

Lerner, A. H., Wallace, P. J., Shea, T., Mourey, A. J., Kelly, P. J., Nadeau, P. A., Elias, T., Kern, C., Clor, L. E., Gansecki, C., et al. (2021). The petrologic and degassing behavior of sulfur and other magmatic volatiles from the 2018 eruption of kīlauea, hawaii: melt concentrations, magma storage depths, and magma recycling. *Bulletin of Volcanology*, 83(6):1–32.

Masotta, M. and Mollo, S. (2019). A new plagioclase-liquid hygrometer specific to trachytic systems. *Minerals*, 9(6):375.

Masotta, M., Mollo, S., Freda, C., Gaeta, M., and Moore, G. (2013). Clinopyroxene–liquid thermometers and barometers specific to alkaline differentiated magmas. *Contributions to Mineralogy and Petrology*, 166(6):1545–1561.

Matthews, S., Shorttle, O., and Maclennan, J. (2016). The temperature of the i celandic mantle from olivine-spinel aluminum exchange thermometry. *Geochemistry, Geophysics, Geosystems*, 17(11):4725–4752.

Matzen, A. K., Baker, M. B., Beckett, J. R., and Stolper, E. M. (2011). Fe–mg partitioning between olivine and high-magnesian melts and the nature of hawaiian parental liquids. *Journal of Petrology*, 52(7-8):1243–1263.

Molina, J., Moreno, J., Castro, A., Rodríguez, C., and Fershtater, G. (2015). Calcic amphibole thermobarometry in metamorphic and igneous rocks: New calibrations based on plagioclase/amphibole al-si partitioning and amphibole/liquid mg partitioning. *Lithos*, 232:286–305.

Mollo, S., Putirka, K., Misiti, V., Soligo, M., and Scarlato, P. (2013). A new test for equilibrium based on clinopyroxene–melt pairs: clues on the solidification temperatures of etnean alkaline melts at post-eruptive conditions. *Chemical Geology*, 352:92–100.

Montierth, C., Johnston, A. D., and Cashman, K. V. (1995). An empirical glass-composition-based geothermometer for mauna loa lavas. *Washington DC American Geophysical Union Geophysical Monograph Series*, 92:207–217.

Mutch, E., Blundy, J., Tattitch, B., Cooper, F., and Brooker, R. (2016). An experimental study of amphibole stability in low-pressure granitic magmas and a revised al-in-hornblende geobarometer. *Contributions to Mineralogy and Petrology*, 171(10):1–27.

Mutch, E. J., Maclennan, J., Shorttle, O., Rudge, J. F., and Neave, D. A. (2021). Dfens: Diffusion chronometry using finite elements and nested sampling.

Neave, D. A., Bali, E., Guðfinnsson, G. H., Halldórsson, S. A., Kahl, M., Schmidt, A.-S., and Holtz, F. (2019). Clinopyroxene–liquid equilibria and geothermobarometry in natural and experimental tholeiites: the 2014–2015 holuhraun eruption, iceland. *Journal of Petrology*, 60(8):1653–1680.

Neave, D. A. and Putirka, K. D. (2017). A new clinopyroxene-liquid barometer, and implications for magma storage pressures under icelandic rift zones. *American Mineralogist*, 102(4):777–794.

ONNX-Runtime-developers (2021). Onnx runtime. https://www.onnxruntime.ai. Version: x.y.z.

pandas development team, T. (2020). pandas-dev/pandas: Pandas.

Petrelli, M. (2021). Introduction to python in earth science data analysis. page 229.

Petrelli, M., Caricchi, L., and Perugini, D. (2020). Machine learning thermo-barometry: Application to clinopyroxene-bearing magmas. *Journal of Geophysical Research: Solid Earth*, 125(9):e2020JB020130.

Pollack, H. N. and Chapman, D. S. (1977). On the regional variation of heat flow, geotherms, and lithospheric thickness. *Tectonophysics*, 38(3-4):279–296.

Powell, R., Holland, T., and Worley, B. (1998). Calculating phase diagrams involving solid solutions via non-linear equations, with examples using thermocalc. *Journal of metamorphic Geology*, 16(4):577–588.

Pritchard, M., Mather, T., McNutt, S. R., Delgado, F., and Reath, K. (2019). Thoughts on the criteria to determine the origin of volcanic unrest as magmatic or non-magmatic. *Philosophical Transactions of the Royal Society A*, 377(2139):20180008.

Pu, X., Lange, R. A., and Moore, G. (2017). A comparison of olivine-melt thermometers based on d mg and d ni: The effects of melt composition, temperature, and pressure with applications to morbs and hydrous arc basalts. *American Mineralogist*, 102(4):750–765.

Pu, X., Moore, G. M., Lange, R. A., Touran, J. P., and Gagnon, J. E. (2021). Experimental evaluation of a new h2o-independent thermometer based on olivine-melt ni partitioning at crustal pressure. *American Mineralogist: Journal of Earth and Planetary Materials*, 106(2):235–250.

Putirka, K. (1999). Clinopyroxene+ liquid equilibria to 100 kbar and 2450 k. *Contributions to Mineralogy and Petrology*, 135(2-3):151–163.

Putirka, K. (2016). Amphibole thermometers and barometers for igneous systems and some implications for eruption mechanisms of felsic magmas at arc volcanoes. *American Mineralogist*, 101(4):841–858.

Putirka, K., Johnson, M., Kinzler, R., Longhi, J., and Walker, D. (1996). Thermobarometry of mafic igneous rocks based on clinopyroxene-liquid equilibria, 0–30 kbar. *Contributions to Mineralogy and Petrology*, 123(1):92–108.

Putirka, K., Ryerson, F., and Mikaelian, H. (2003). New igneous thermobarometers for mafic and evolved lava compositions, based on clinopyroxene+ liquid equilibria. *American Mineralogist*, 88:1542–1554.

Putirka, K. D. (2005). Igneous thermometers and barometers based on plagioclase+ liquid equilibria: Tests of some existing models and new calibrations. *American Mineralogist*, 90(2-3):336–346.

Putirka, K. D. (2008). Thermometers and barometers for volcanic systems. *Reviews in mineralogy and geochemistry*, 69(1):61–120.

Putirka, K. D. (2017). Down the crater: where magmas are stored and why they erupt. *Elements*, 13(1):11–16.

Rasmussen, D. J., Plank, T. A., Roman, D. C., and Zimmer, M. M. (2022). Magmatic water content controls the pre-eruptive depth of arc magmas. *Science*, 375(6585):1169–1172.

Rasmussen, D. J., Plank, T. A., Wallace, P. J., Newcombe, M. E., and Lowenstern, J. B. (2020). Vapor-bubble growth in olivine-hosted melt inclusions. *American Mineralogist: Journal of Earth and Planetary Materials*, 105(12):1898–1919.

Ridolfi, F. (2021). Amp-tb2: An updated model for calcic amphibole thermobarometry. *Minerals*, 11(3):324.

Ridolfi, F. and Renzulli, A. (2012). Calcic amphiboles in calc-alkaline and alkaline magmas: thermobarometric and chemometric empirical equations valid up to 1,130° c and 2.2 gpa. *Contributions to Mineralogy and Petrology*, 163(5):877–895.

Ridolfi, F., Renzulli, A., and Puerini, M. (2010). Stability and chemical equilibrium of amphibole in calc-alkaline magmas: an overview, new thermobarometric formulations and application to subduction-related volcanoes. *Contributions to Mineralogy and Petrology*, 160(1):45–66.

Roeder, P. and Emslie, R. (1970). Olivine-liquid equilibrium. *Contributions to Mineralogy and Petrology*, 29(4):275–289.

Rout, S. S., Blum-Oeste, M., and Wörner, G. (2021). Long-term temperature cycling in a shallow magma reservoir: insights from sanidine megacrysts at taápaca volcano, central andes. *Journal of Petrology*.

Rudnick, R. L. (1995). Making continental crust. *Nature*, 378(6557):571–578.

Ryan, C. G., Griffin, W. L., and Pearson, N. J. (1996). Garnet geotherms: Pressure-temperature data from Cr-pyrope garnet xenocrysts in volcanic rocks. *Journal of Geophysical Research: Solid Earth*, 101(B3):5611–5625.

Schmidt, M. W. (1992). Amphibole composition in tonalite as a function of pressure: an experimental calibration of the al-in-hornblende barometer. *Contributions to mineralogy and petrology*, 110(2-3):304–310.

Scruggs, M. A. and Putirka, K. D. (2018). Eruption triggering by partial crystallization of mafic enclaves at chaos crags, lassen volcanic center, california. *American Mineralogist: Journal of Earth and Planetary Materials*, 103(10):1575–1590.

Shamloo, H. I. and Till, C. B. (2019). Decadal transition from quiescence to supereruption: petrologic investigation of the lava creek tuff, yellowstone caldera, wy. *Contributions to Mineralogy and Petrology*, 174(4):1–18.

Sisson, T. and Grove, T. (1993). Temperatures and h 2 o contents of low-mgo high-alumina basalts. *Contributions to Mineralogy and Petrology*, 113(2):167–184.

Stock, M. J., Bagnardi, M., Neave, D. A., Maclennan, J., Bernard, B., Buisman, I., Gleeson, M. L., and Geist, D. (2018). Integrated petrological and geophysical constraints on magma system architecture in the western galápagos archipelago: insights from wolf volcano. *Geochemistry, Geophysics, Geosystems*, 19(12):4722–4743.

Stock, M. J., Humphreys, M. C., Smith, V. C., Isaia, R., and Pyle, D. M. (2016). Late-stage volatile saturation as a potential trigger for explosive volcanic eruptions. *Nature Geoscience*, 9(3):249–254.

Sudholz, Z., Yaxley, G., Jaques, A., and Chen, J. (2021). Ni-in-garnet geothermometry in mantle rocks: a high pressure experimental recalibration between 1100 and 1325° c. *Contributions to Mineralogy and Petrology*, 176(5):1–16.

Sugawara, T. (2000). Empirical relationships between temperature, pressure, and mgo content in olivine and pyroxene saturated liquid. *Journal of Geophysical Research: Solid Earth*, 105(B4):8457–8472.

Szymanowski, D., Wotzlaw, J.-F., Ellis, B. S., Bachmann, O., Guillong, M., and von Quadt, A. (2017). Protracted near-solidus storage and pre-eruptive rejuvenation of large magma reservoirs. *Nature Geoscience*, 10(10):777–782.

Till, C. B. (2017). A review and update of mantle thermobarometry for primitive arc magmas. *American Mineralogist*, 102(5):931–947.

Toplis, M. (2005). The thermodynamics of iron and magnesium partitioning between olivine and liquid: criteria for assessing and predicting equilibrium in natural and experimental systems. *Contributions to Mineralogy and Petrology*, 149(1):22–39.

Walker, B. A., Klemetti, E. W., Grunder, A. L., Dilles, J. H., Tepley, F. J., and Giles, D. (2013). Crystal reaming during the assembly, maturation, and waning of an eleven-million-year crustal magma cycle: thermobarometry of the aucanquilcha volcanic cluster. *Contributions to Mineralogy and Petrology*, 165(4):663–682.

Wan, Z., Coogan, L. A., and Canil, D. (2008). Experimental calibration of aluminum partitioning between olivine and spinel as a geothermometer. *American Mineralogist*, 93(7):1142–1147.

Wang, X., Hou, T., Wang, M., Zhang, C., Zhang, Z., Pan, R., Marxer, F., and Zhang, H. (2021). A new clinopyroxene thermobarometer for mafic to intermediate magmatic systems. *European Journal of Mineralogy*, 33(5):621–637.

Waters, L. E. and Lange, R. A. (2015). An updated calibration of the plagioclase-liquid hygrometer-thermometer applicable to basalts through rhyolites. *American Mineralogist*, 100(10):2172–2184.

Wells, P. R. (1977). Pyroxene thermometry in simple and complex systems. *Contributions to mineralogy and Petrology*, 62(2):129–139.

Wieser, P. E., Edmonds, M., Gansecki, C., Maclennan, J., Jenner, F. E., Kunz, B., Antoshechkina, P., Trusdell, F., and Lee, R. L. (2022). Explosive activity on kīlauea's lower east rift zone fueled by a volatile-rich, dacitic melt. *Geochemistry, Geophysics, Geosystems*, 23(2):e2021GC010046.

Wieser, P. E., Edmonds, M., Maclennan, J., Jenner, F. E., and Kunz, B. E. (2019a). Crystal scavenging from mush piles recorded by melt inclusions. *Nature communications*, 10(1):1–11.

Wieser, P. E., Lamadrid, H., Maclennan, J., Edmonds, M., Matthews, S., Iacovino, K., Jenner, F. E., Gansecki, C., Trusdell, F., Lee, R. L., et al. (2021). Reconstructing magma storage depths for the 2018 kılauean eruption from melt inclusion co2 contents: the importance of vapor bubbles. *Geochemistry, Geophysics, Geosystems*, 22(2):e2020GC009364.

Wieser, P. E., Vukmanovic, Z., Kilian, R., Ringe, E., Holness, M. B., Maclennan, J., and Edmonds, M. (2019b). To sink, swim, twin, or nucleate: A critical appraisal of crystal aggregation processes. *Geology*, 47(10):948–952.

Williams, M. J., Schoneveld, L., Mao, Y., Klump, J., Gosses, J., Dalton, H., Bath, A., and Barnes, S. (2020). pyrolite: Python for geochemistry. *Journal of Open Source Software*, 5(50):2314.

Winpenny, B. and Maclennan, J. (2011). A partial record of mixing of mantle melts preserved in icelandic phenocrysts. *Journal of Petrology*, 52(9):1791–1812.

Wood, B. J. and Banno, S. (1973). Garnet-orthopyroxene and orthopyroxene-clinopyroxene relationships in simple and complex systems. *Contributions to Mineralogy and Petrology*, 42(2):109–124.

Zhang, J., Humphreys, M. C., Cooper, G. F., Davidson, J. P., and Macpherson, C. G. (2017). Magma mush chemistry at subduction zones, revealed by new melt major element inversion from calcic amphiboles. *American Mineralogist: Journal of Earth and Planetary Materials*, 102(6):1353–1367.